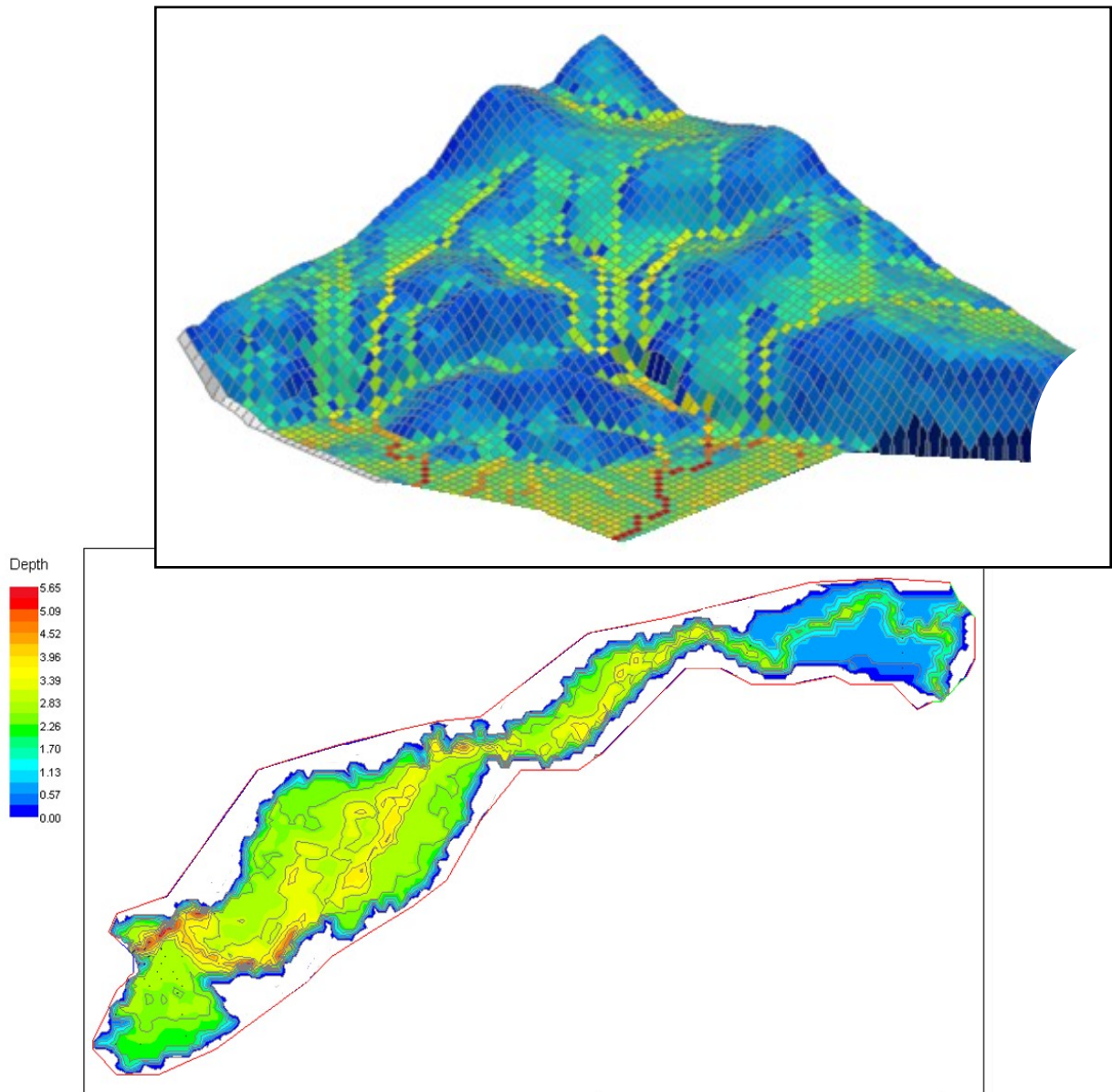


Investigating the protection of Fairbourne village from flooding



Supplement to the report presented to
Arthog Community Council

Graham Hall

January 2022

CONTENTS

1. Introduction	3
2. Sea conditions	5
Climate change	9
3. Estuary system	11
Estuary tidal model	16
4. Hillslope system	22
Soils	23
River routing	26
Hillslope runoff model	28
5. Marine system	32
Wave overtopping	35
6. Coastal lowland system	41
Hydrological model	47
7. Summary	58
References	59

1. INTRODUCTION

The objective of this supplement is to give a straightforward explanation of the science underlying the flood risk to Fairbourne, and the value and limitations of the computer models used in flood forecasting for the area. The text is directed towards the non-specialist reader, so that they may be better informed when taking part in discussions about future plans for the village.

It has been stated that the village of Fairbourne is at serious and increasing risk of severe flooding from the sea, the Mawddach estuary, rivers draining the hills around the village, and localised flooding which develops on the coastal lowland during storm events. It appears to be the intention of Gwynedd County Council to abandon and demolish the village at some time shortly after 2045. This decision has been widely reported by the national media.

A survey was recently carried out by Arthog Community Council to obtain the views of Fairbourne residents to the proposed plans for the village (Arthog Community Council, 2021). It is clear that there is a feeling by residents that they have not been adequately involved in discussions:

- “It’s unacceptable for residents not to be consulted and yet to be impacted so fundamentally in terms of lives, families and property by the decisions taken.”
- “Having attended the multi-agency meeting in the village hall, residents are ‘stone walled’, not listened to, and told what to do without our views being considered. I feel this is why some people may not engage as they feel it is useless.”

Residents are concerned that Fairbourne is being selected for decommissioning without adequate justification:

- “We are aware that there are many communities at risk of coastal erosion and rising sea level. We have the impression that Fairbourne is being singled out for abandonment when in fact other towns/villages in the same area have been more affected by storms and rising sea level. We would argue the village should be treated fairly and appropriately according to the facts and the risks.”
- It has been stressed at public meetings and acknowledged by Natural Resources Wales that local knowledge is important. Is Gwynedd County Council just relying on consultants with computers?”

It is known that the Fairbourne area has been historically affected by flooding (fig.1).

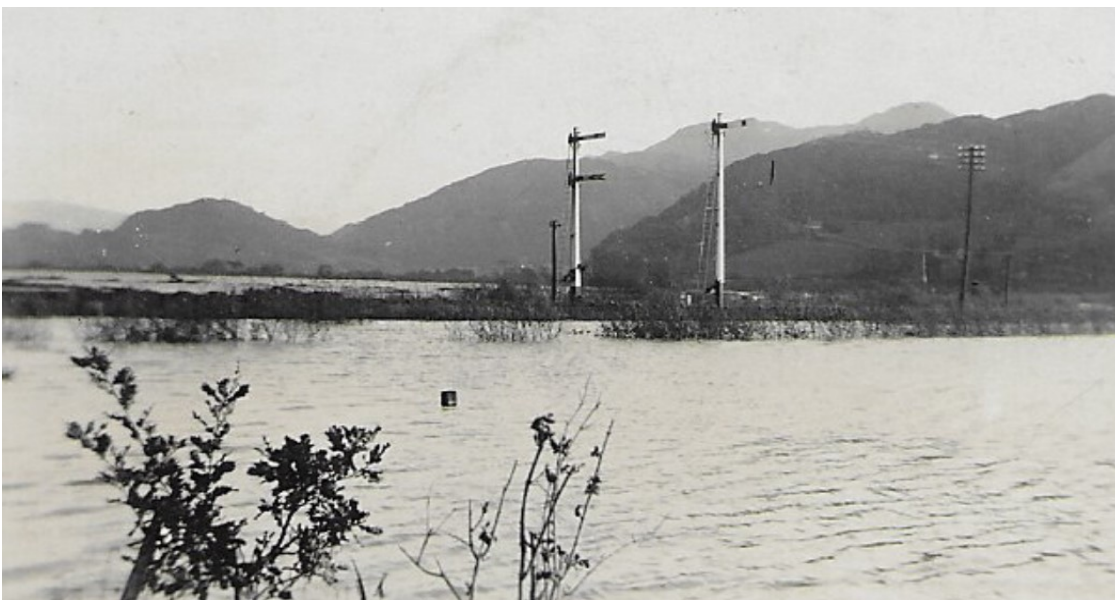


Figure 1:

Flooding at
Morfa Mawddach,
1927

As a consequence of floods such as the 1927 event, flood defence embankments were constructed along the estuary shore and alongside the Afon Arthog. No widespread flooding has occurred in the area since the construction of these embankments. The structures were strengthened and increased in height during the 2016 Fairbourne flood alleviation scheme and now provide a high degree of protection (fig.2).



Figure 2:

Flood defence embankment alongside the tidal mouth of the Afon Arthog. A drainage ditch discharges through a culvert under the embankment, enclosed by the rectangle of fence.



Figure 3:

Tidal gate at the outlet of the culvert, which opens at low tide to allow outflow of drainage water from Arthog Bog and adjacent farmland.

Fairbourne nevertheless remains vulnerable to flooding from a series of small rivers and streams which cross the coastal lowland to discharge into the estuary through tidal gates (fig.3).

A revised flood protection scheme is proposed for Fairbourne, which incorporates the existing sea wall, estuary and railway embankments, along with a new section of embankment to be built across agricultural land immediately to the east of the village. The objective of the scheme is to eliminate the risk of flooding from the Afon Henddol which flows around Fairbourne, and of surface water flooding from the coastal lowland. The scheme would also greatly reduce the length of estuary embankment that would need to be maintained and perhaps upgraded to protect the village.

A series of questions have been addressed in the accompanying feasibility study for the proposed new flood defence scheme, and will be further investigated here:

- Is there any risk of failure of the sea defences between Friog and Fairbourne? Are the sand and shingle storm beach deposits along this section of the coastline stable, or subject to erosion or deposition?
- What volume of water is likely to wash over the sea defences through wave overtopping during a worst case storm event?
- Is the estuary embankment around the north of Fairbourne village of sufficient height to prevent overtopping from the estuary during a worst case storm event? Is the embankment of sufficiently substantial construction to withstand damage and prevent throughflow at times of high water level in the estuary?
- Would the village be adequately protected against flooding from the Afon Henddol and surface water accumulating on the coastal lowland during a worst case storm event?
- Can drainage water within the Fairbourne flood protection boundary be discharged effectively into the Mawddach estuary during and after a worst case storm event?

The methodology for answering these questions will generally begin by examining field data collected in Fairbourne and the wider local area. Computer modelling will then investigate any increase in flood risk which might occur as a result of climate change up to the year 2065.

2. SEA CONDITIONS

Much of the argument for the abandoning of Fairbourne is centred around predictions of sea level rise which may lead to flooding from the sea and estuary. In this section, the main scientific factors affecting current and future sea levels are considered.

Tides are fundamental to coastal processes. A graph of tidal heights at Barmouth for a typical month is shown in fig.4.

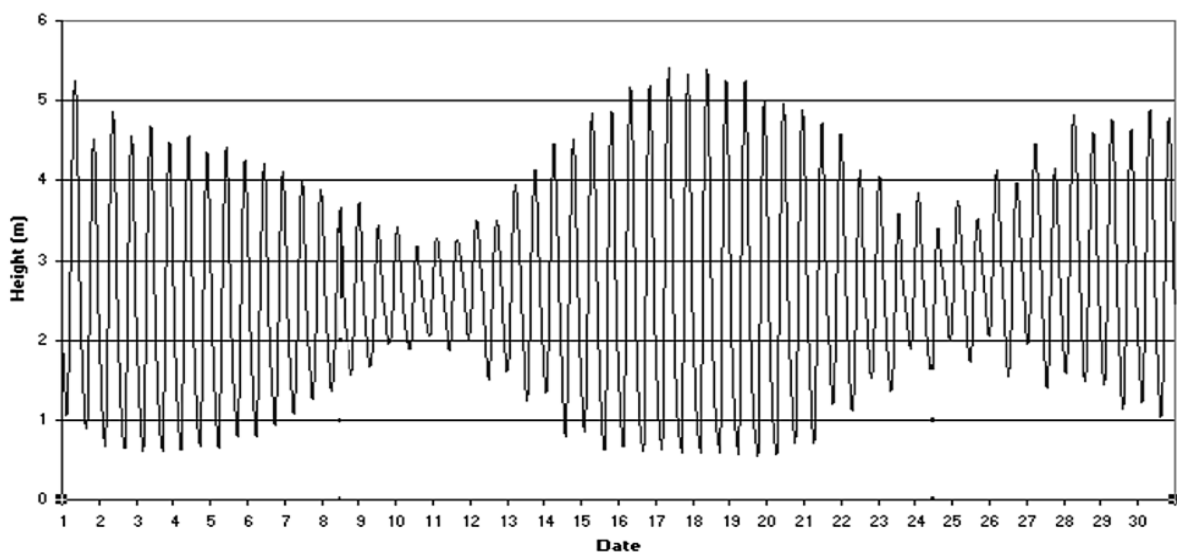


Figure 4: Typical tidal data for Barmouth

The tidal graph shows complex variations during the month. The most obvious feature is the approximately twice-daily high tide caused by interaction between the Earth and moon. A high tide occurs at the point closest to the moon due to gravitational attraction, and furthest away from the moon due to rotational inertia acting on the water body where the gravitational force from the moon is lowest (fig.5).

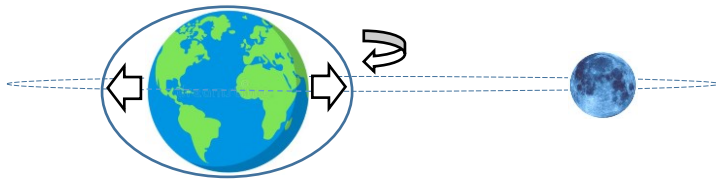


Figure 5:
Tidal influence of the moon.

During each month, variations between periods of spring and neap tide are caused by the alignment of the Earth, moon and sun. Every fortnight, the sun and moon lie in approximately the same line, so that tidal effects are increased. This produces particularly high spring tides (fig.6).

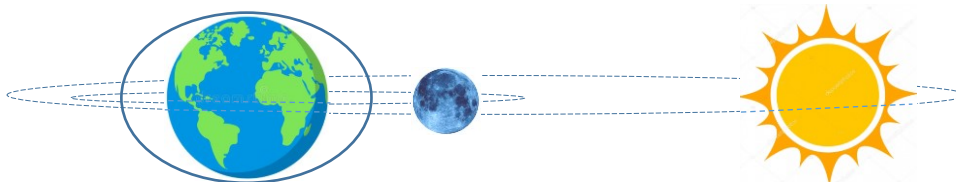


Figure 6:
Spring tides produced by a sun-moon alignment.

A week after the spring tides, the moon and sun will be positioned at right angles when observed from the Earth. The cumulative tidal effect is reduced, and lower neap tides are produced (fig.7).

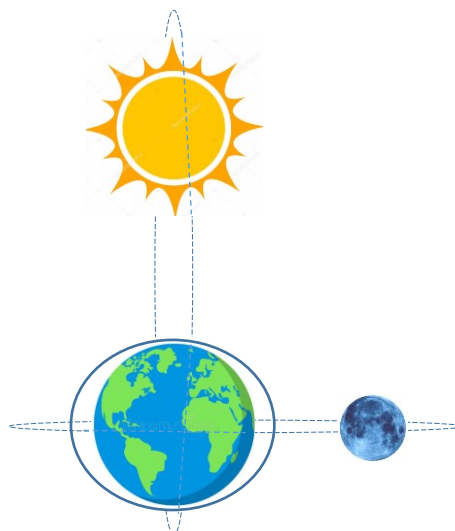


Figure 7:
Neap tides produced by the sun and moon aligned at right angles relative to the earth.

These normal astronomical tides occur as bodies of water move through the oceans in response to the gravitational effects of the moon and sun. However, the water flows are often heavily constrained by the distribution of land masses. Maximum tidal heights vary considerably around the coast of Britain (fig.8). These are highest where converging coasts create a funnel shape into which tidal flows are concentrated. The greatest tidal ranges are found in the Severn estuary, Morecambe Bay and the English Channel. On more open sections of coast, the tidal range is less extreme. The current maximum daily tidal range for spring tides at Barmouth is 5.5m.

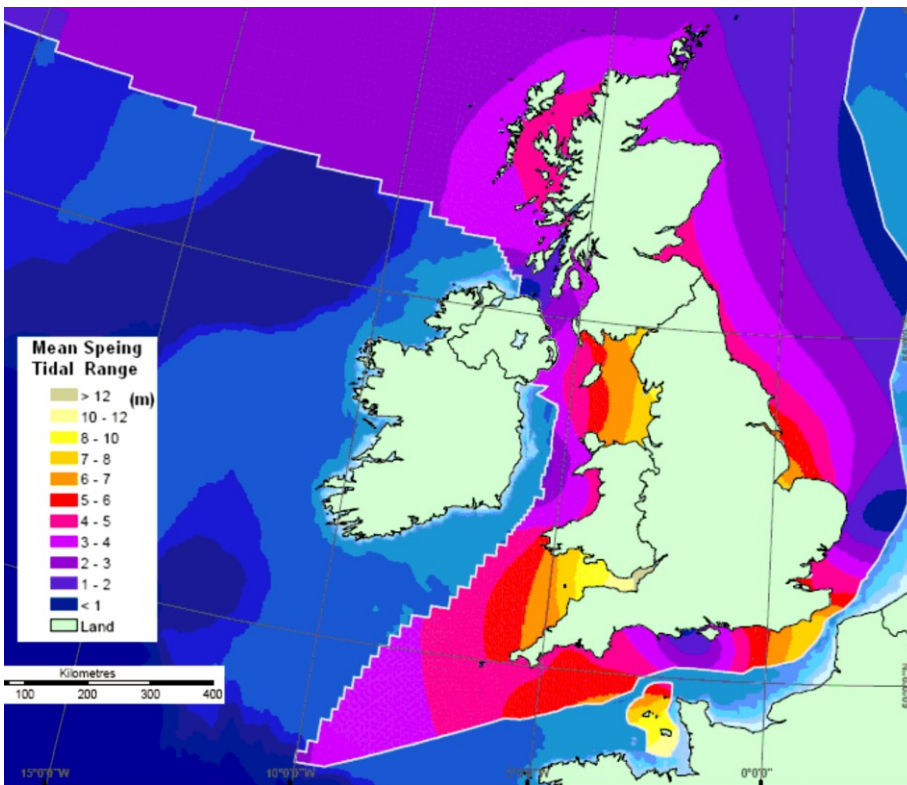


Figure 8:
Variations in tidal range around the coast of Britain.
(Ahmadian, Morris, & Falconer, 2010).

High spring tides alone are unlikely to cause coastal flooding. The risk becomes greater when the water height is increased by a storm surge.

Surges are generated by low pressure weather systems, with the most extreme being hurricanes. The low atmospheric pressure causes a rise in the sea surface beneath the storm. Descending storm winds depress the mass of water immediately below the storm centre, which is then pushed outwards by the circulating winds to create the surge (fig.9).

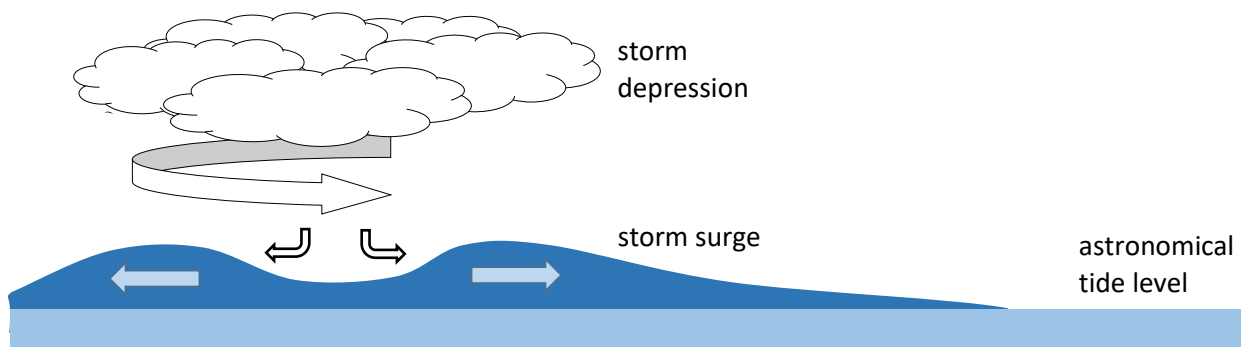


Figure 9: Creation of a storm surge beneath a low pressure weather system.

Once generated, storm surges travel across the ocean in the same manner as the tides. Fig.10 shows a computer model produced using DELFT 3D software to illustrate a worst case scenario of a hurricane-force storm travelling through the Irish Sea (Deltares, 2017). The Irish Sea is a semi-enclosed body of water, so the associated surge is relatively weak. The maximum surge height is predicted to be 1m above the level of the astronomical tide. The storm surge may contribute to coastal flooding if it should occur during a maximum spring tide.

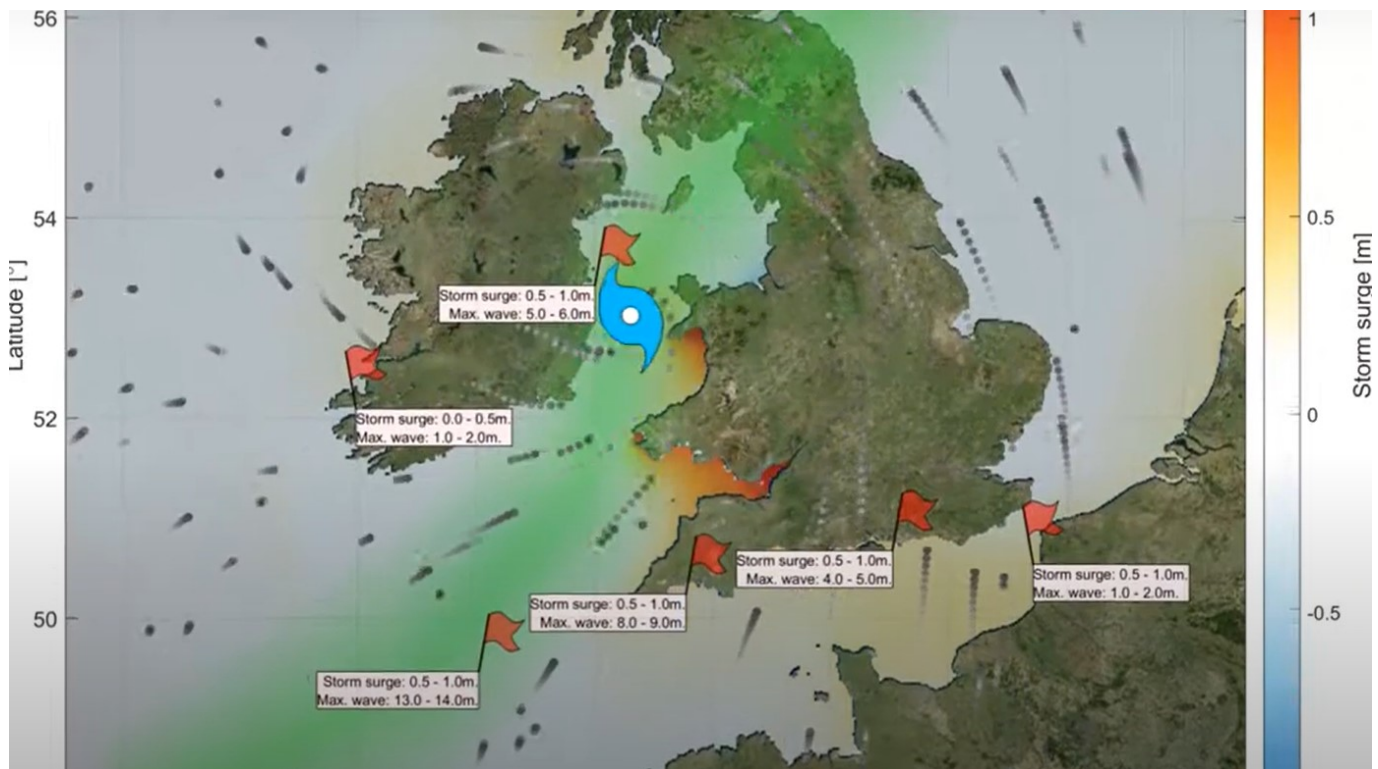


Figure 10: Storm surge as a consequence of a hurricane-force storm travelling through the Irish Sea.

A further risk for coastal flooding is the action of waves. There are three main factors that affect wave formation: wind velocity, fetch, and duration. Fetch is the distance over the water that the wind can blow uninterrupted. The greater the wind velocity, the longer the fetch, and the greater duration the wind blows, then the more energy is converted to waves and the bigger the waves. However, if wind speed is slow, the waves will be small. It takes all three factors acting together to create big waves.

The Irish Sea is sheltered, with only relatively narrow connections to the south along St. George's Channel and to the north along the North Channel, so the majority of waves are locally generated. The wind direction leading to the largest waves at Fairbourne is from the south west, where the fetch direction extends out into the Atlantic. Modelling predicts that the maximum wave height above specified tidal height for the central Irish Sea would be 8m (fig.11). This storm wave height would be expected to occur once in 50 years.

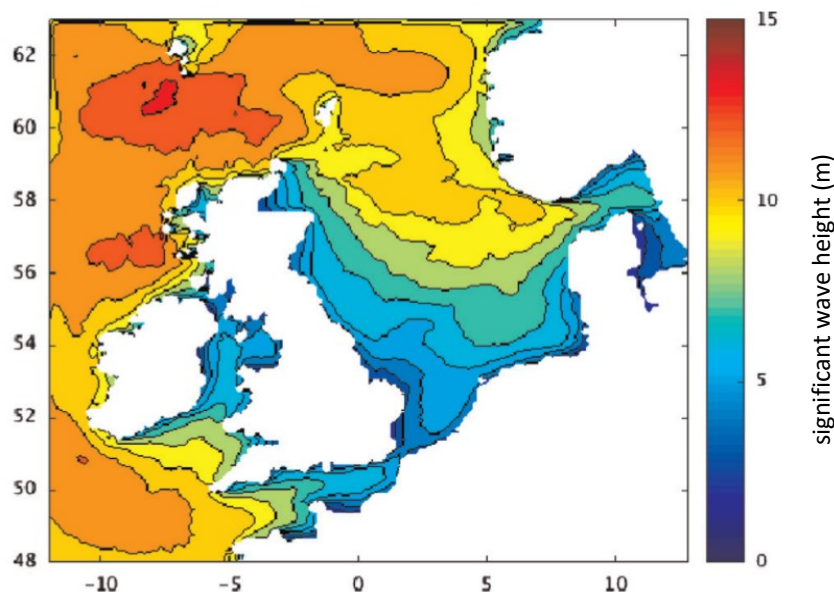


Figure 11: Distribution of extreme wave heights with a 50 year return period (Bricheno, Wolf, & Aldridge, 2015).

Observations of waves in Cardigan Bay were compiled by Thompson, Karunarathna, & Reeve (2017) for a series of severe storms which caused extensive damage to the promenade in Aberystwyth during January 2014. It was found that waves reached a maximum height of 7m above specified tidal height under extreme storm conditions offshore from Aberporth (fig.12).

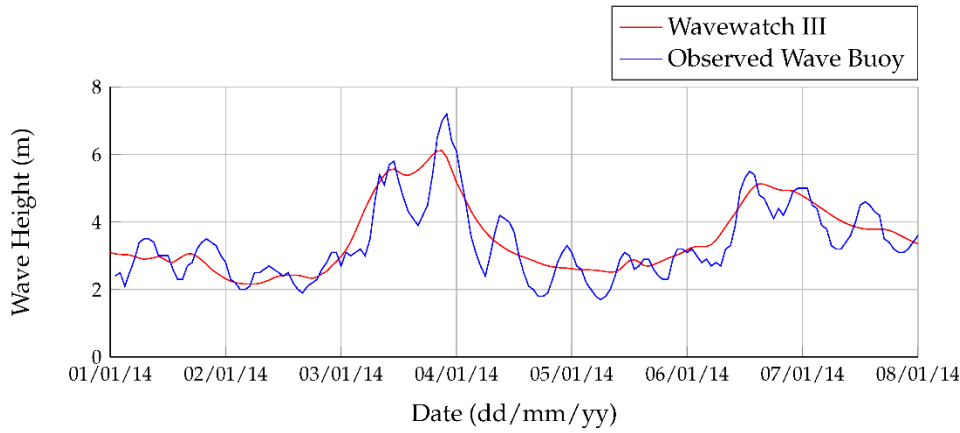


Figure 12:

Wave heights in Cardigan Bay at an offshore recording point (blue) during storm conditions. A computer model (red) is shown for comparison. (Thompson et al. 2017)

Wave height tends to reduce on moving from open sea towards the coastline. The maximum wave height close to the coast at Fairbourne is unlikely to exceed 6m.

Climate change

Phillips, Thomas and Morgan (2017) have compiled data from the Barmouth tidal gauge in order to investigate the current trend in sea level. Graphs are shown in fig.13.

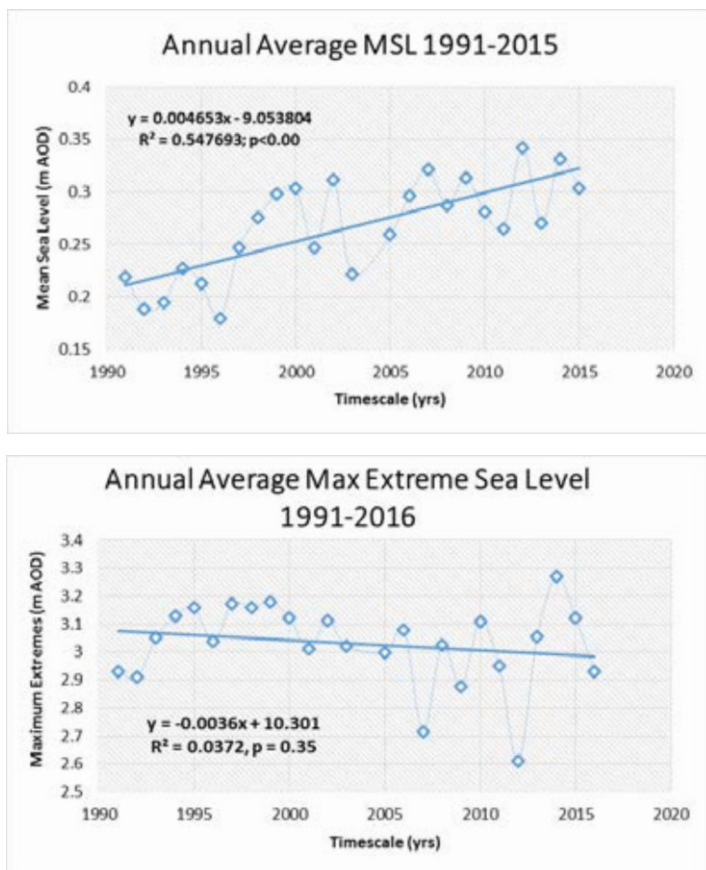


Figure 13:

Average and maximum sea levels recorded at Barmouth railway bridge for the period 1991-2016. (Phillips, Thomas and Morgan, 2017).

Best-fit straight lines applied to the data give somewhat ambiguous results. Whilst mean sea level has risen by approximately 0.1m between 1990 and 2015, the maximum sea level has remained approximately constant during this period.

An examination of storm surges shows considerable variation from year to year, depending on the relatively random occurrence of severe storms. However, the average surge height seems to have remained approximately constant over the period 1991 – 2016 (fig.14).

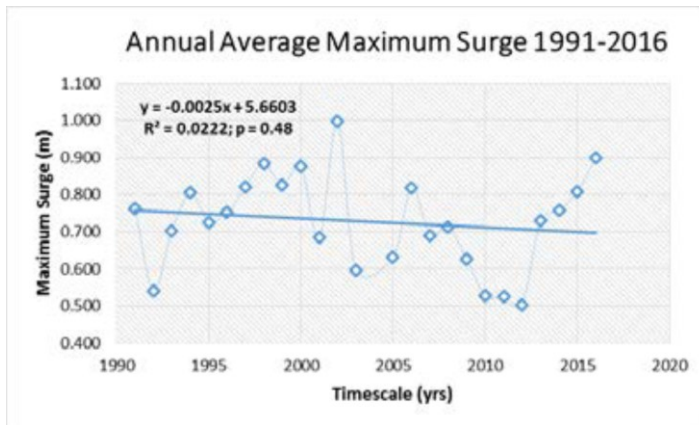


Figure 14: Maximum storm surge heights recorded at Barmouth railway bridge for the period 1991-2016. (Phillips, Thomas and Morgan, 2017).

On the basis of these observations, no significant increase in storm surge height in excess of current sea conditions would be expected at Fairbourne for the period up to 2065. An increase in mean sea level of approximately 0.5m is predicted, with the risk of coastal flooding primarily dependent on the maximum tidal height during a spring tide corresponding with a storm surge.

Models have been produced for future sea level rise based on a variety of assumptions relating to carbon emissions. These assumptions are in turn dependent on political actions by governments around the world, and wide variations are seen in the results of the models. A widely accepted sea level model is UKCP09 (fig.15), giving a maximum likely sea level rise up to 2065 of 0.3m.

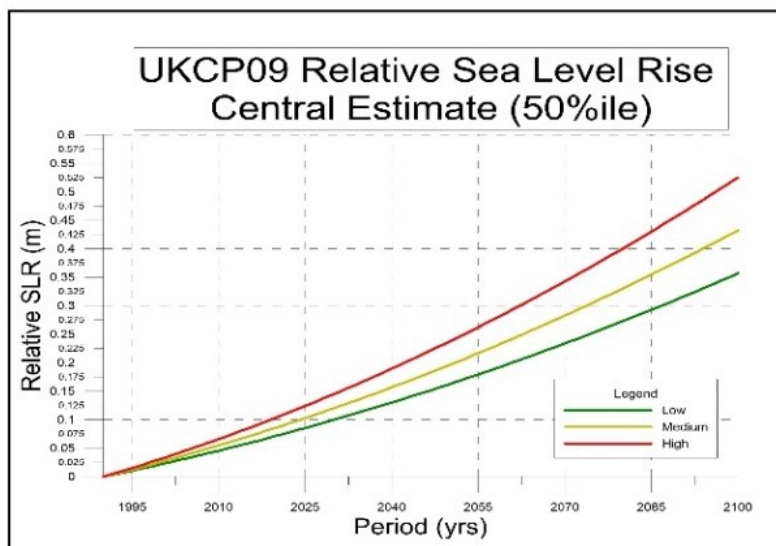


Figure 15: UKCP09 predictions for relative change in sea level for different carbon emissions scenarios. (UK Government, 2014)

Based on the published data, it appears reasonable to assume a maximum increase in mean sea level at Fairbourne of 0.5m up to the year 2065. There is no strong evidence to suggest that maximum excess wave height, including storm surge, will increase from the current extreme value of 8m estimated for the central area of the Irish Sea. A maximum in-shore excess wave height of 6m at Fairbourne is a reasonable assumption up to the year 2065.

3. ESTUARY SYSTEM

To investigate the risk to Fairbourne of flooding from the Mawddach estuary, it is necessary to examine the response of the estuary to storm events.

The course of the estuary between the sea at Barmouth and the upper tidal limit near Dolgellau is shown in figures 16 and 17.



Figure 16: The lower and middle basins of the Mawddach estuary.



Figure 17: The upper estuary basin. Arrows indicate the approximate tidal limits.

Water depth recorders were installed on the rivers Mawddach and Wnion a short distance downstream from the tidal limits, to investigate tidal effects in the upper basin (Hall, 2008). A typical recording is shown in fig.18.

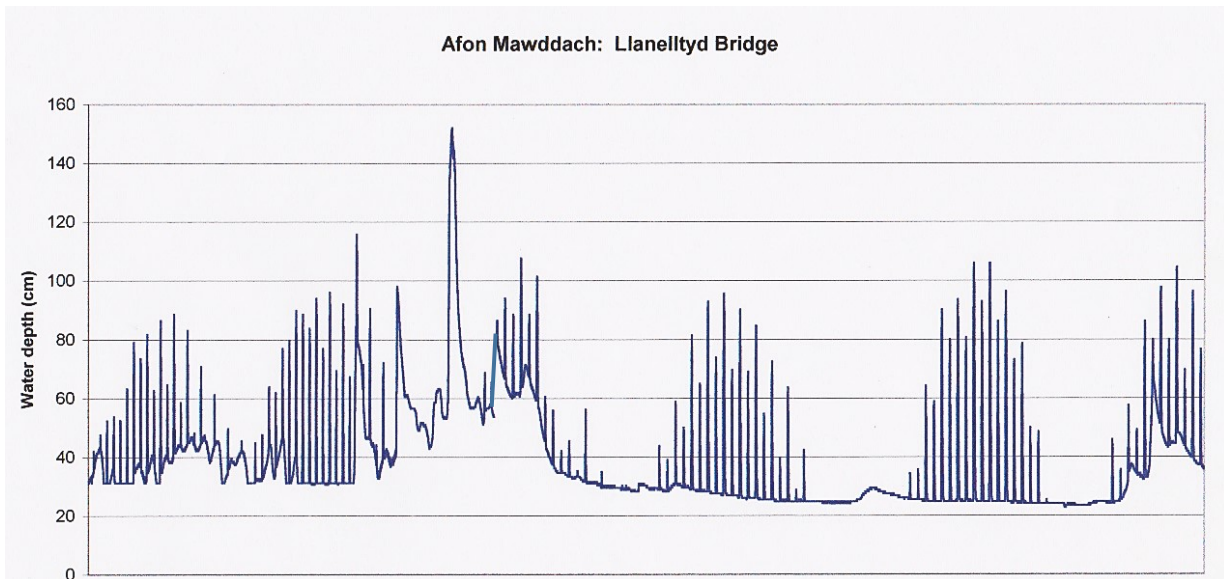


Figure 18: Hydrograph for the Afon Mawddach near the tidal limit.

The underlying pattern of the hydrograph is produced by river flow, which shows a steady base level of around 30cm. A storm flood event was recorded when the river level rose briefly to 150cm. Superimposed on the river discharge are a series of twice-daily tidal peaks which closely correspond to tidal peaks measured at Barmouth. It is apparent that tidal flows only reach the rivers at the head of the estuary during spring cycles, and the lower neap tides are not represented.

A comparison of the absolute heights of tidal peaks at Barmouth and on the rivers at the estuary head indicate that the tidal flow loses height as it travels along the length of the estuary (fig.19). This is in contrast to estuaries such as the Severn, where the tidal peak increases in height as it travels upstream.

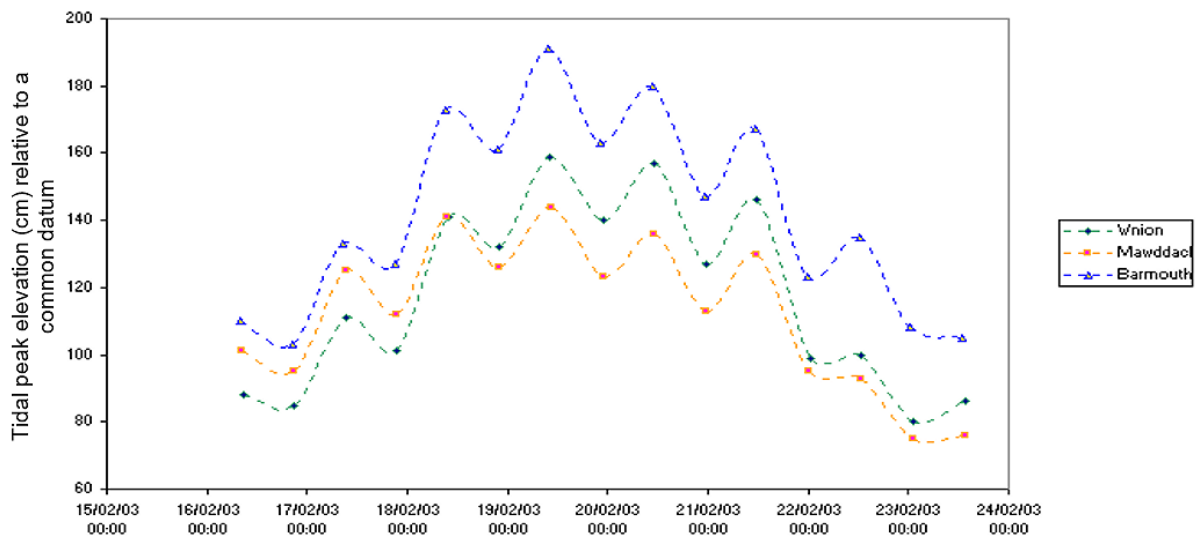


Figure 19: Tidal maximum heights at the estuary mouth and at the estuary head.

The reduction in tidal height along the Mawddach estuary is mainly due to water entering wetlands within the upper basin (fig.20), where it is temporarily stored until the tide falls again.



Figure 20: Wetlands in the upper estuary basin. (left) *Phragmites australis* reed beds (right) Wet woodland of willow, alder and birch above reed beds.

A hydrograph recorder was installed at Penmaenpool bridge (fig.21), close to the headland which marks the boundary between the upper and middle estuary basins.



Figure 21:

(above) Location of the hydrograph recorder at Penmaenpool bridge.

(below) Example hydrograph record.



Tidal peaks are very prominent. A significant feature is the asymmetric shape of the peaks, with a rapid tidal rise which inundates the estuary wetlands, then a more gradual fall as the wetlands drain on a falling tide.

The mountainous region is regularly affected by storm events, which can create floods on the rivers Mawddach and Wnion (fig.22).



Figure 22: Flooding on the Afon Mawddach near the tidal limit at Llanelltyd.

This often leads to extensive flooding of low lying agricultural land in the upper estuary basin between Dolgellau and Penmaenpool (fig.23).



Figure 23: Flooded fields near Penmaenpool.

In the lower estuary basin during a major river flood event, at low tide there is only a limited effect on the width of the water channels flowing between sand banks. Salt marsh alongside the lower basin is exposed in much the same way as it is during times of low river flow.

It can be concluded that the lower estuary basin is so strongly dominated by tidal flows that river flooding has no effect on the maximum tidal level recorded at Barmouth railway bridge. At high tide, river floodwater remains in temporary storage within the upper and middle estuary basins, and is gradually released when the tide falls. A model for estuary water flows at a time of river flooding is given in fig.24.

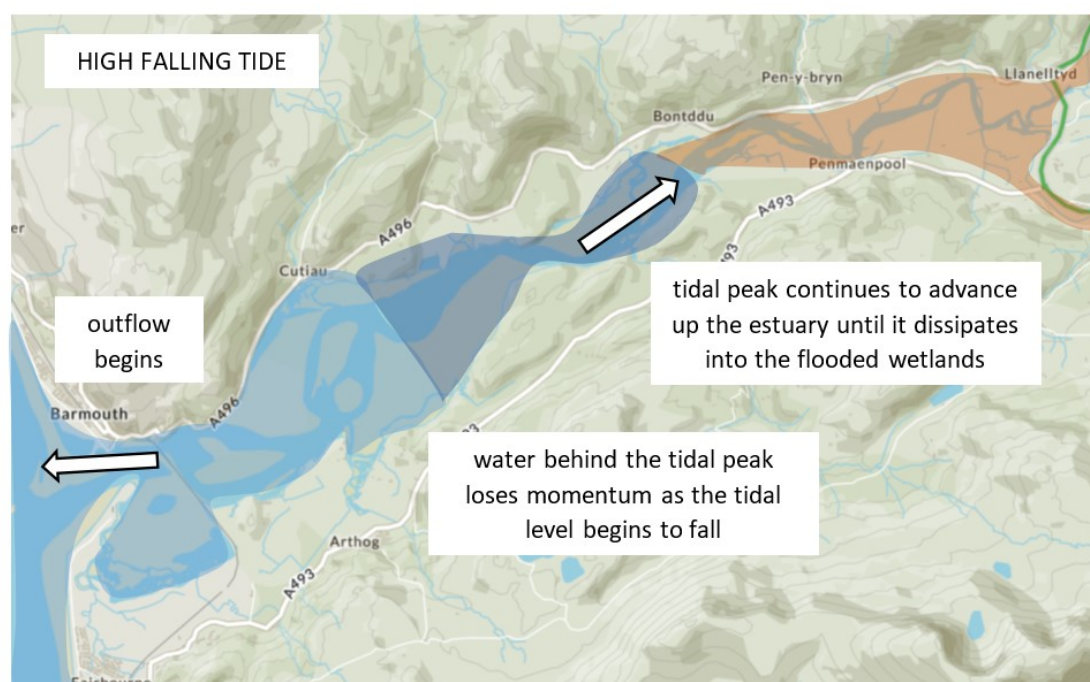
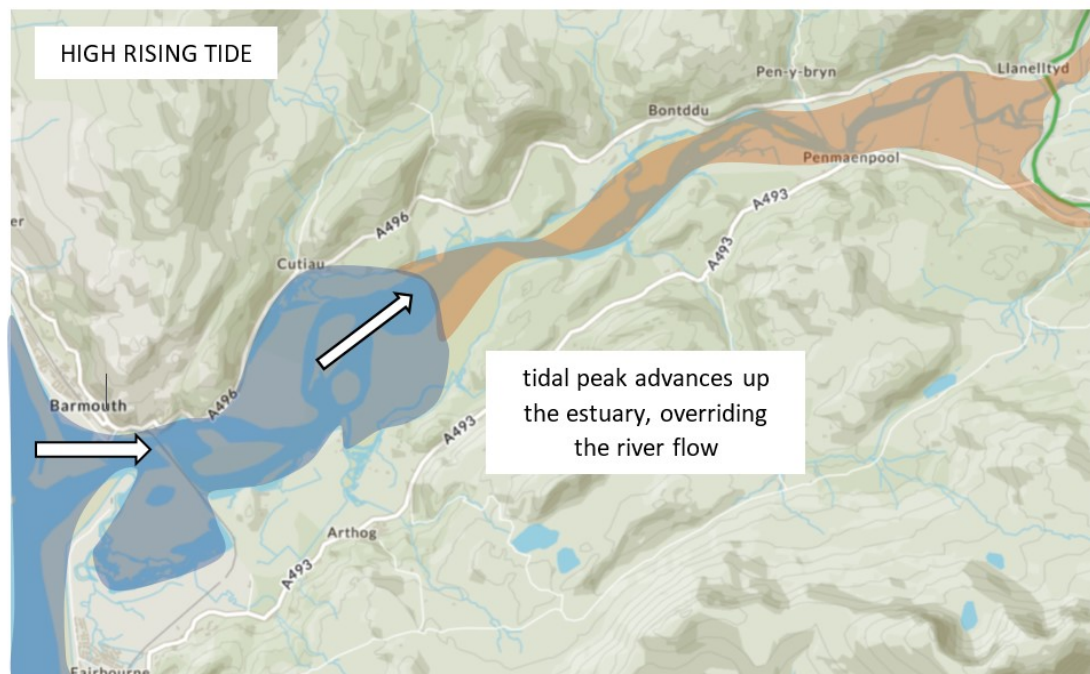
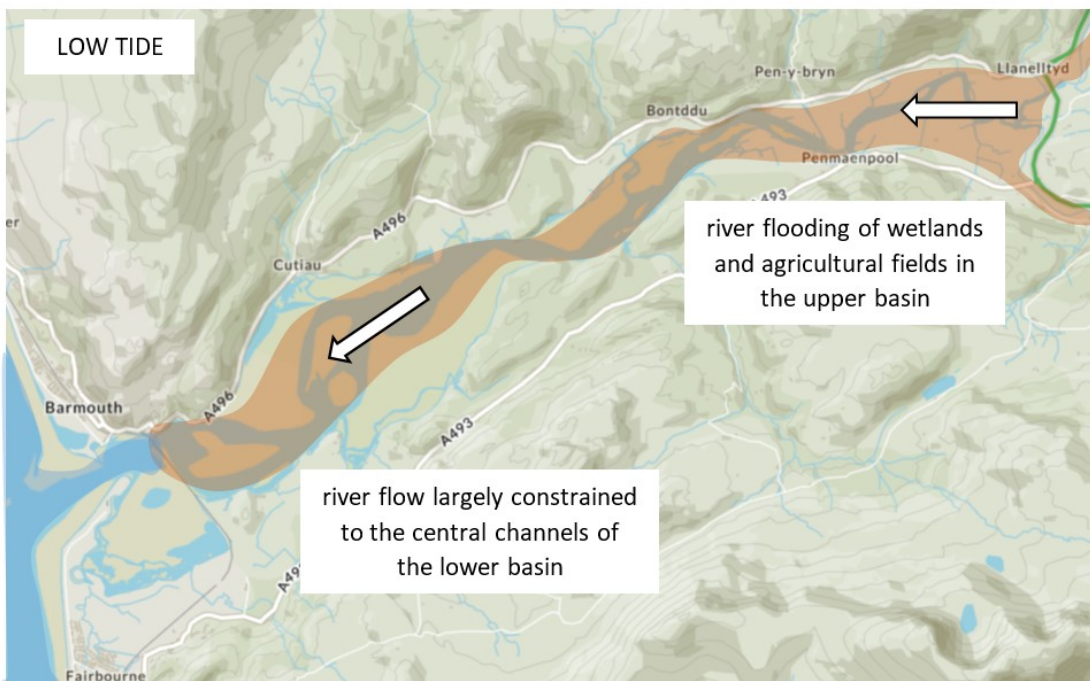


Figure 24:

Model for river and tidal flows during a period of flooding at the head of the estuary.

From the timings of hydrograph peaks, it is found that the tidal peak takes approximately 35 minutes to travel the length of the estuary from Barmouth to Llanelltyd (fig.25).

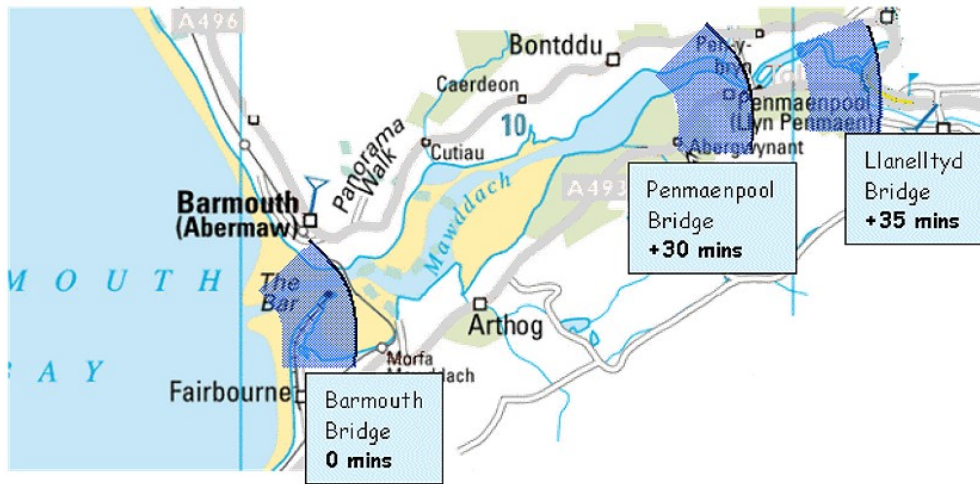


Figure 25: Passage time for tidal peaks along the Mawddach estuary.

Estuary tidal model

The assumed pattern for the discharge of flood water in the Mawddach estuary system was tested by comparison with a RIVER 2D computer model. The model is set up by creating a grid of points at which the elevations of the estuary bed are recorded. The grid is extended to surrounding areas of land within the flood plain.

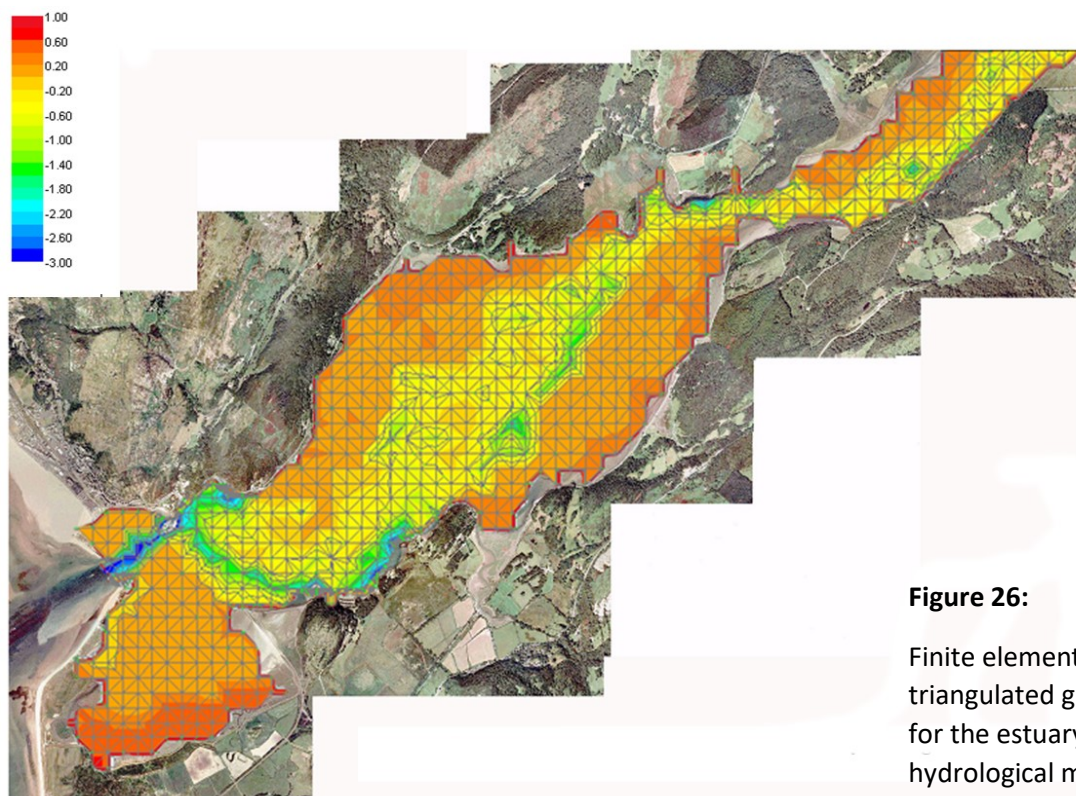


Figure 26:
Finite element triangulated grid for the estuary hydrological model.

The RIVER 2D program models the estuary water flow in a series of short time steps, which in total can simulate one or more tidal cycles. Inflows from rivers can be specified, and may vary with time to represent the occurrence of a flood event. Rising and falling tidal heights at the mouth of the estuary are specified, along with the occurrence of any tidal surge.

The area of the estuary model is divided into a number of elements, with the scalar water surface elevation and the vector flow velocity computed at each time step. The basic controlling equation is the conservation of mass:

$$\left[\begin{array}{c} \text{change} \\ \text{in stored} \\ \text{volume} \end{array} \right] = \left[\begin{array}{c} \text{inflow} \\ \text{volume} \end{array} \right] - \left[\begin{array}{c} \text{outflow} \\ \text{volume} \end{array} \right]$$

which can be expressed mathematically as:

$$\frac{\partial H}{\partial t} + \frac{\partial q_x}{\partial x} + \frac{\partial q_y}{\partial y} = 0$$

where: H is water surface elevation, t is time, and q_x and q_y are discharge components in the x and y directions.

Water will flow away from points with higher water surface elevation, as a result of hydrostatic pressure created by the differences in hydraulic head.

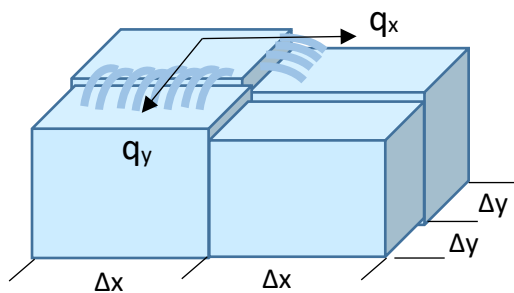


Figure 27:

Water flow due to differences in hydraulic head.

The flow velocity, however, is determined by the momentum of the water. The flow is fastest when momentum is high. An equation keeps an account of changes in momentum:

$$\left[\begin{array}{c} \text{change in} \\ \text{momentum} \end{array} \right] = \left[\begin{array}{c} \text{change due} \\ \text{to bed slope} \end{array} \right] - \left[\begin{array}{c} \text{loss due to} \\ \text{bed friction} \end{array} \right] - \left[\begin{array}{c} \text{loss due to} \\ \text{turbulence} \end{array} \right]$$

Changes in the elevation of the channel bed will alter the momentum of the overlying column of water. A fall in the channel bed provides gravitational potential energy which can be converted into kinetic energy to increase the momentum of the flow. Conversely, a rise in the bed will remove kinetic energy and momentum from the flow (fig.28). Changes in momentum are again computed as components in the x and y grid directions.

Momentum can be removed from the water flow by friction with the channel bed. For a sand bed, this may be the result of transferring energy to sand grains to create advancing dunes and ripples. Greater amounts of energy can be removed when the water flow passes through and over salt marsh vegetation at high tide. The program allows different frictional parameters to be applied to sand banks and salt marshes within the estuary.

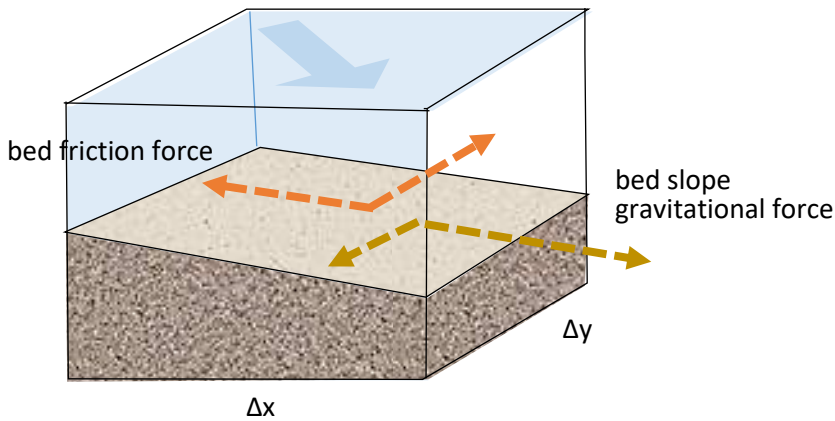


Figure 28:
River bed factors affecting water flow.

A more complex aspect of water flow is turbulence. This is a rotational motion which can be created in various situations, for example: when water flows over rapids or a weir; when fast flowing water is forced to change direction around a bend in the channel; or when water flows through tall vegetation such as reed beds.

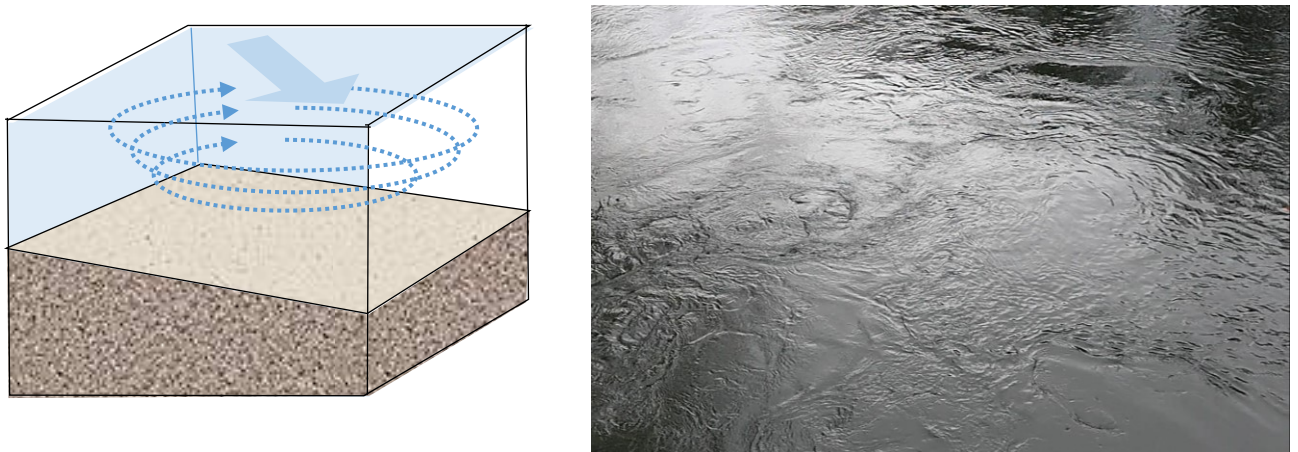


Figure 29: (left) Turbulence counteracting the forwards motion of a water flow.
(right) Turbulence generated in the tidal Afon Wnion near Dolgellau.

The RIVER 2D program has effective functions for simulating the wetting and drying of saltmarshes during tidal cycles. It offers opportunities to investigate the effects of salt marsh, reed beds and wet woodlands in enhancing temporary water storage. The model incorporates an eddy viscosity coefficient which is used in simulating the turbulent shear stresses which are high for water flows through dense, tall vegetation but low for unimpeded flows across grassland. The model indicates that reed beds and wet woodland can increase water depth on the floodplain by up to 60cm in comparison to grassland, with a consequent increase in temporary storage and reduction in tidal height in the upper basin.

In initial models, the tidal flows through the estuary mouth were modelled by simply varying the external sea level as a sine curve of 4m amplitude. Whilst this produced realistic patterns of inflow and outflow for the lower estuary basin, the time taken for the passage of a tidal peak up the estuary was an order of magnitude too slow.

The program was modelling the passive gravitational movement of an elevated water mass on the surface of a body of stationary water. It became clear that the real physical situation involves the dynamic inflow of substantial water volumes at high velocities through the whole depth of the water column at the estuary mouth during a rising tide. A revision of the estuary mouth boundary condition was carried out, to model rising tides as transient inflows varying sinusoidally between 0 and $4\,000\text{m}^3\text{s}^{-1}$. Falling tides continued to be modelled by sinusoidally varying water level elevation at the estuary mouth. This combination of boundary conditions produced satisfactory timings for the movement of tidal peaks up the estuary.

The sequence begins with water inflow through the estuary mouth on a rising tide. (fig.30). Water flow reaches 5ms^{-1} through the estuary mouth at the time of maximum water level increase at mid-tide.

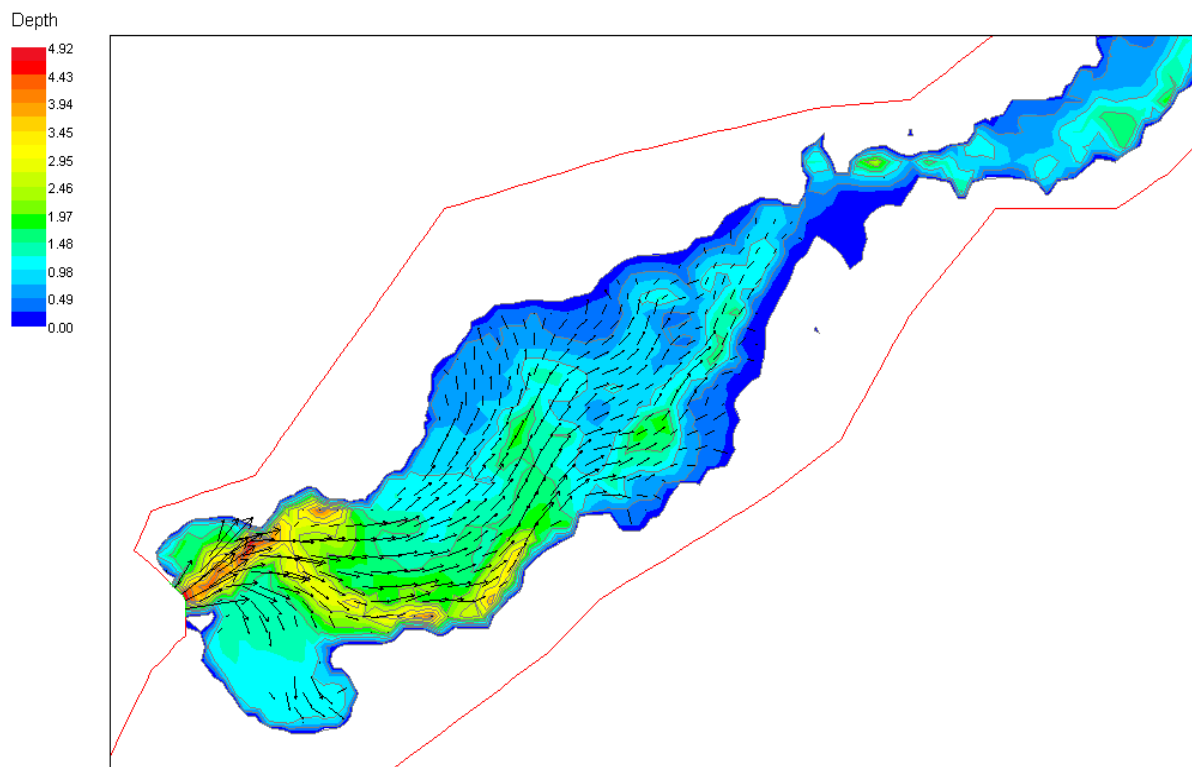


Fig.30: Water flow through the estuary mouth at the period of maximum inflow on a rising tide.

Fig.31 shows the tidal inflow travelling up the estuary through the channel constriction between the lower and middle basins at Farchynys, where velocities reach 3ms^{-1} .

As the tide turns and begins to fall, outflow begins at the estuary mouth (fig.32). Fast flow occurs within the channel system, with slower drainage from the extensive tidal flats of the lower estuary basin.

Channel water levels show a progressive decline upstream through the estuary, eventually reaching the upper basin where drainage occurs from the salt marshes and reed beds (fig.33).

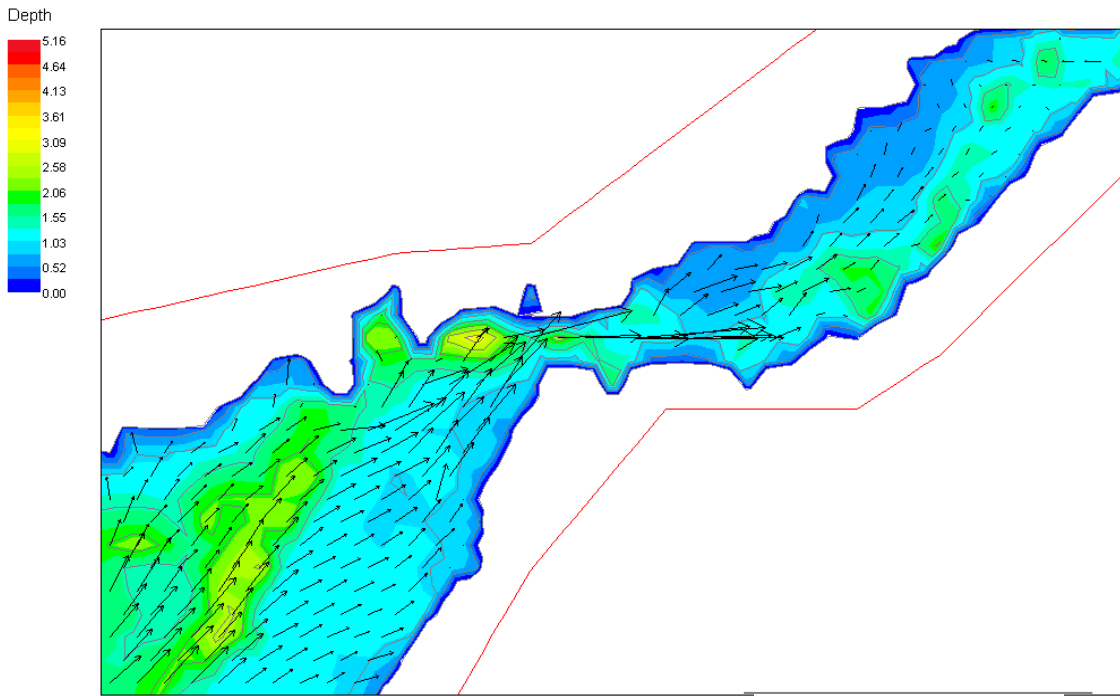


Figure 31:

Peak tidal inflow travelling up the estuary from the lower to the middle basin.

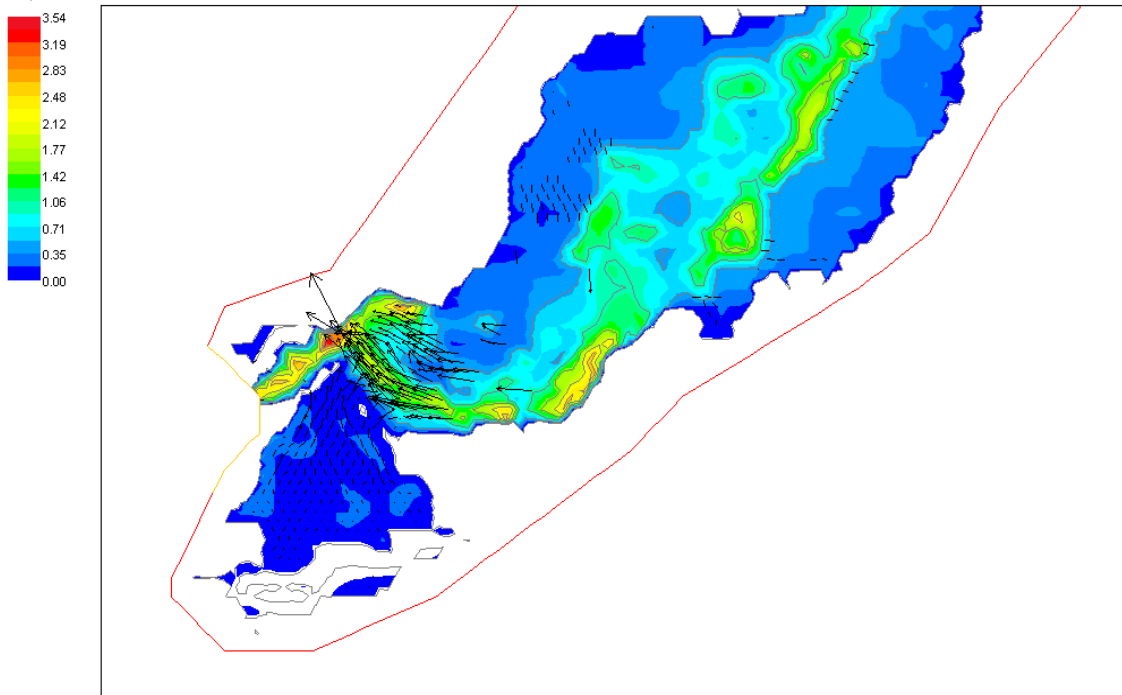


Figure 32:

Outflow beginning at the estuary mouth on a falling tide, with outflow from salt marshes north of Fairbourne.

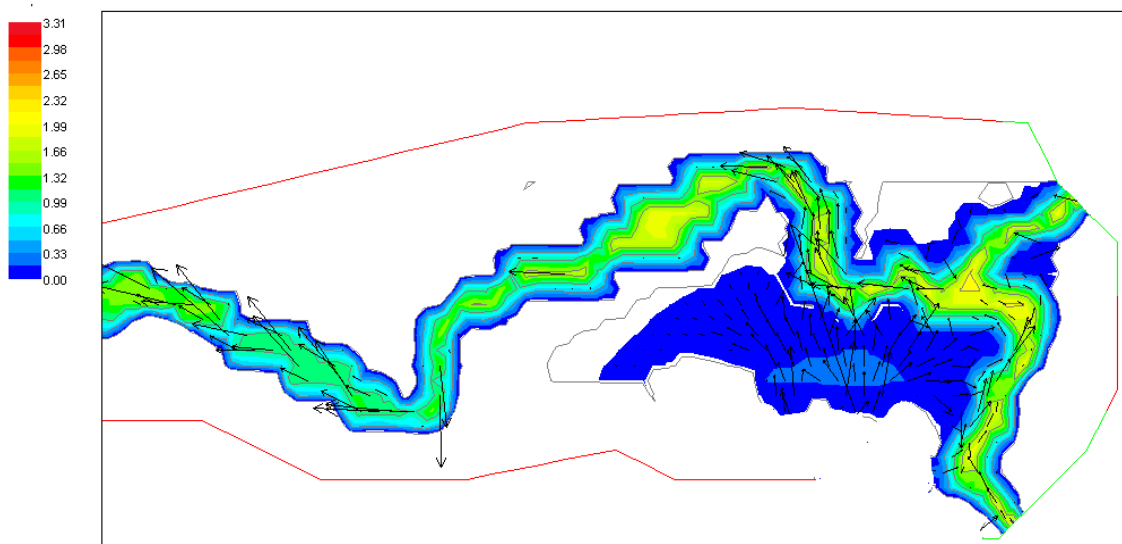


Figure 33:

Drainage beginning from the salt marshes and reed beds in the upper basin.

The simulated hydrograph for Penmaenpool is given in fig.34. In comparison with the actual hydrograph recorded at Penmaenpool bridge, this shows a similar asymmetric pattern with rapid water rise on the incoming tide followed by a more gradual, roughly exponential fall as water flows out of temporary storage in the reed beds and salt marshes of the upper estuary basin.

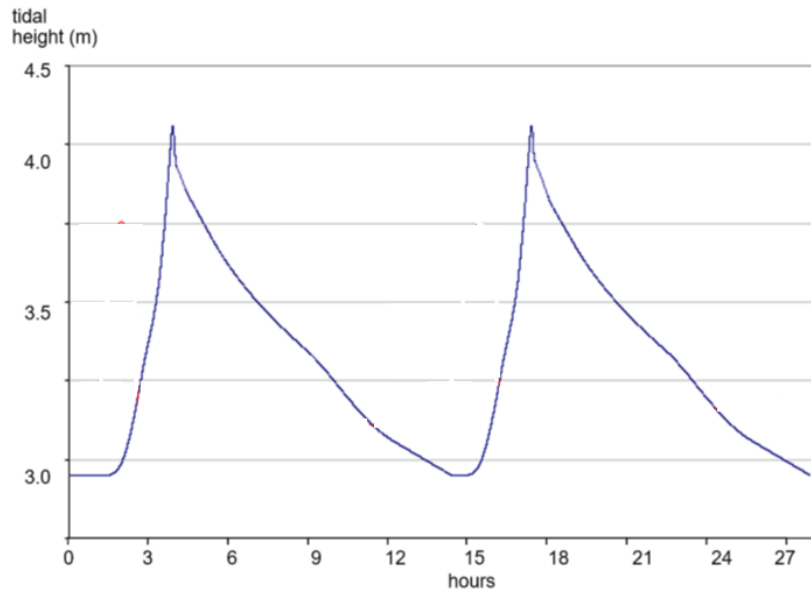


Figure 34:
Simulated hydrograph for Penmaenpool Bridge.

The whole-estuary model is considered to give a satisfactory representation of tidal flows. It appears very unlikely that the water height against the estuary flood embankment at Fairbourne could exceed the combined tidal and flood surge height at the estuary mouth. Sea waves rapidly dissipate within the enclosed and sheltered waters of the estuary, particularly during shallow tidal flow across the extensive salt marsh.

It is predicted that the maximum water height against the Fairbourne embankment for the year 2065 would be produced by a maximum 6m spring tide combined with a maximum storm surge of 2m, giving a total of 8m above chart datum.

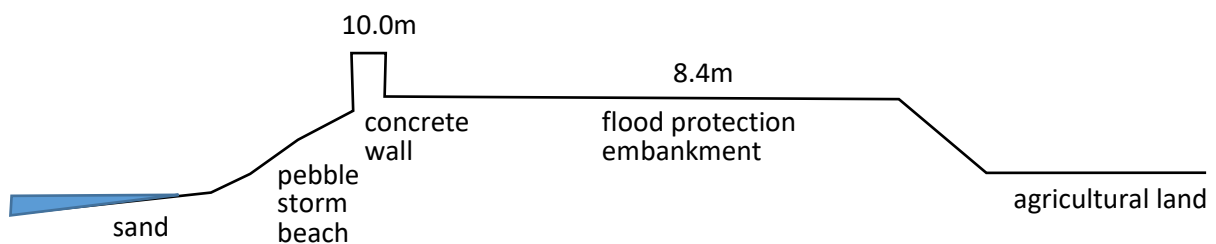


Figure 35: Heights of land components above Chart Datum

Surveying indicates that the height of the Fairbourne embankment is above the predicted maximum water level, but the freeboard of 0.4m is small. It would be advisable to raise the height of the section of flood embankment north of Fairbourne village by 1m as a precautionary measure at some time before 2065.

4. HILLSLOPE SYSTEM

It has been suggested that Fairbourne is at serious risk from flood water descending from the hills to the south of the village. The objective in this section is to examine the mechanisms of hillslope runoff, and to estimate the maximum flood discharges for the Afon Henddol (fig.36) and Afon Morfa under worst case storm conditions as predicted for the year 2065. These water volumes will then be used as inputs to a hydrological model for the coastal lowland around Fairbourne village.



Figure 36: The Afon Henddol in the Einion valley above Friog.

Hillslope runoff takes place after rainfall. This may occur by water flowing across the ground surface, or as shallow throughflow within the soil layer. It is not uncommon for the majority of hillslope discharge to be in the form of shallow throughflow, with water released from springs at the base of a hillside, or discharged directly into a stream channel.

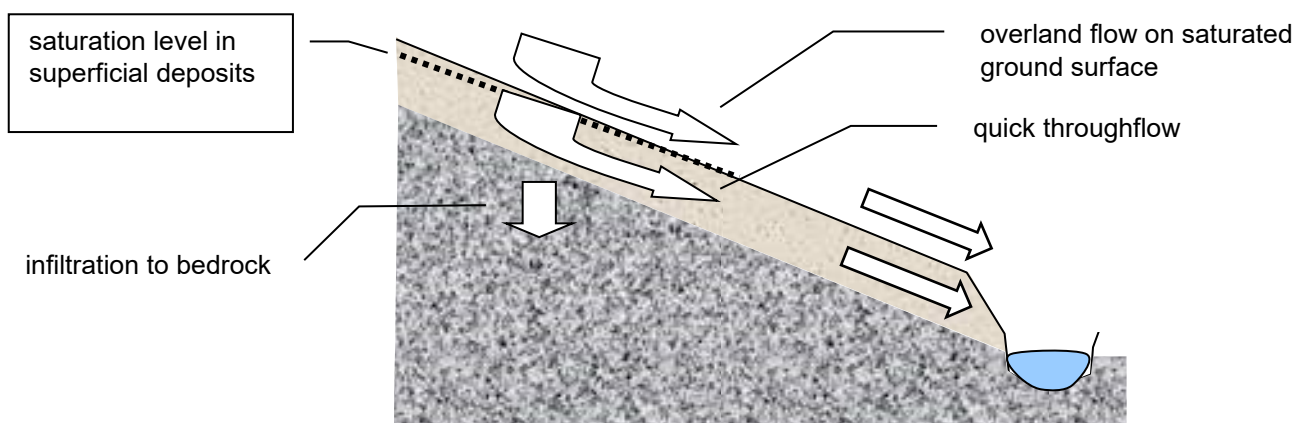


Figure 37: Mechanisms of hillslope runoff after rainfall.

An extreme example of shallow throughflow in glacial deposits is shown in fig.38. The water flow has reduced the mechanical strength within the layer of superficial deposits, leading to slope failure and a landslide.



Figure 38:

Shallow throughflow in glacial deposits which led to a slope failure and landslip, Bethesda.

Surface runoff of storm rainfall can occur when the soil and other superficial deposits become saturated with groundwater, perhaps as a result of several days of continuous rainfall. Further rainwater cannot enter the soil. Alternatively, an extreme storm may deliver rainfall faster than the rate at which water can percolate into unsaturated soil.



Figure 39:

Overland flow as a result of an intense thunderstorm at Trawsfynydd.

Hillslope runoff is a crucial factor affecting flooding. If rainfall is absorbed into the soil and subsoil and then slowly released into a river over several days, the flood risk downstream will be low. However, if the same volume of rainfall quickly reaches a river by overland flow or rapid throughflow, then the river level will rise suddenly and could cause serious flooding downstream.

Soils

Hillslope runoff is strongly dependent on the hydrological characteristics of the soil and subsoil:

- the thickness of these layers;
- their porosity, which determines the amount of water which can be stored;
- their hydraulic conductivity, which determines how rapidly water can enter and leave.

A wide range of soils are found in the Mawddach area, varying greatly in their hydrological properties. Some examples are given below.



A. Humic ranker on hard igneous rock



B. Brown podzolic soil on weathered igneous rock



C. Stagnohumic gley on glacial till



D. Cambic gley on Upper Cambrian shale

Figure 40: Soil types commonly found in the Mawddach catchment.

Ranker soils occur where there is almost no input of mineral material from the hard bedrock. The profile shows a thin layer of poorly decomposed peat lying directly on the solid rock surface.

Brown earth soils are deep and well drained. The upper A horizon consists of well-rotted plant material. Below is the B horizon composed of mineral particles, rich in iron and showing a brown colouration.

Podzolic soils show sharply contrasting soil horizons. The A horizon is dark brown or black and composed of acid humus. Below is a white or bleached horizon from which iron and other bases have been leached by downwards percolating groundwater.

Brown podzolic soils are intermediate between brown earths and podzols, and show a smaller amount of downwards leaching.

Gley soils result from waterlogging. The activity of soil microorganisms is prevented and plant material fails to decompose completely. This gives rise to peat accumulation if growth of vegetation continues.

Cambic soils are poorly developed soils lying on bed rock at shallow depth. Where the bed rock is impermeable, gleying can occur.

When modelling hillslope storm runoff for this project, the HOST (Hydrology Of Soil Types) classification system produced by the Institute of Hydrology is used. Soil profiles are divided into a series of classes (fig.41) with known hydrological responses under storm conditions.

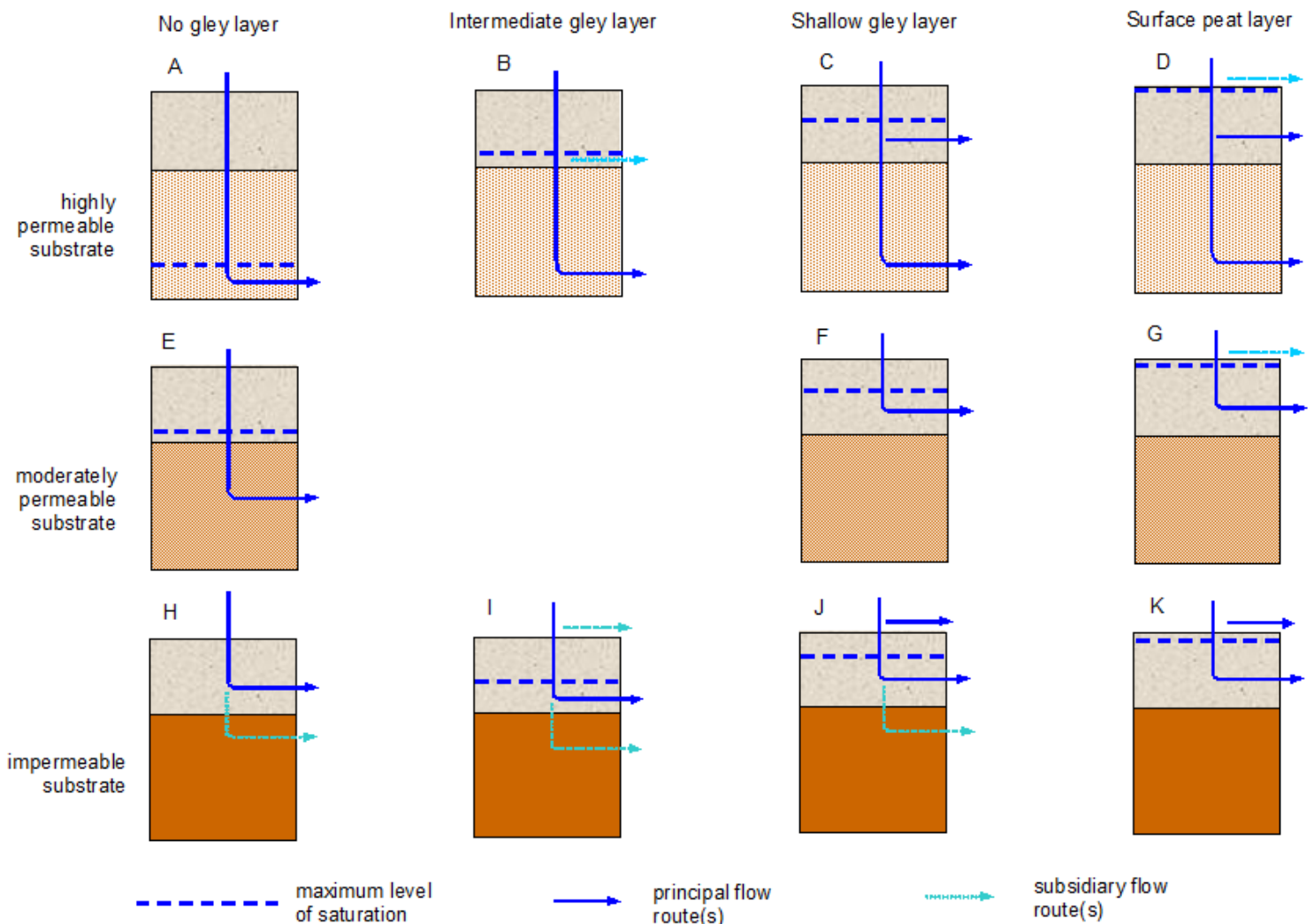


Figure 41: HOST classification of soil types.

The HOST classification depends on two factors:

- The permeability of the material underlying the soil. This forms the three rows of the chart.
- The height of the water table. This forms the four columns of the chart.

Both of these factors can be determined from published map data, without the need to carry out soil sampling at every location in the field:

The permeability of the material underlying the soil is dependent on the geology of the bedrock. For example, hard igneous rocks have low permeability, thinly bedded sedimentary rocks such as shales have an intermediate permeability, whilst superficial deposits such as glacial or estuarine sands have high permeability.

The level of the water table can be predicted according to the location of a site. The soil is likely to be wet, with a high water table, if it receives downslope water flow from a large area. The soil is also likely to be wet if the ground is level or has only a gentle slope. Drier soils tend to occur on steeper slopes, and where there is only a small catchment area providing an inflow of water. A measure of the wetness at any point is given by the Kirkby index (Bevan, 1997):

$$\text{wetness} = \ln(a / \tan \beta)$$

where **a** is upslope contributing area and **β** is slope angle (fig.42).

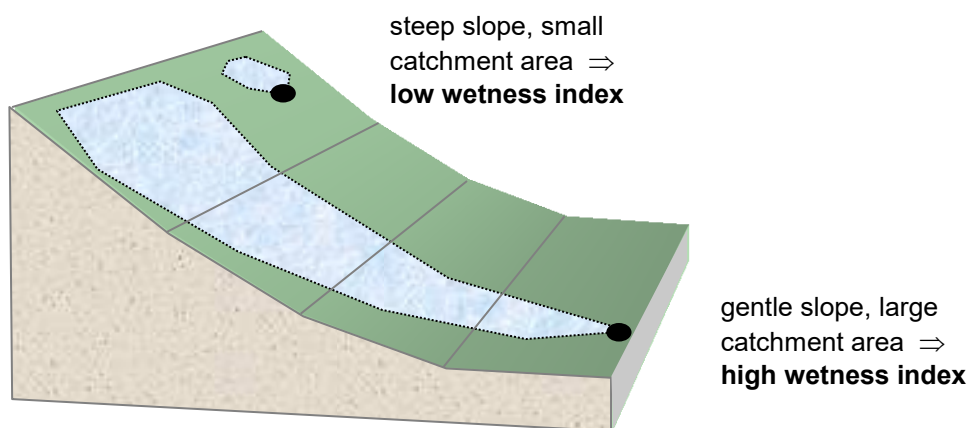


Figure 42: Factors determining the Kirkby wetness index.

The HOST soil type at any location, and its hydrological properties, can therefore be predicted from the underlying geology and the location of the site on the hillslope, as provided by geological and topographical map data.

River routing

Once hillslope runoff reaches a stream, it will be routed through the river network to the coast. As in the case of the estuary tidal flows discussed earlier, the rate at which water moves through the river system will depend on the gradient of the channel, the frictional resistance of the bed, and the amount of water turbulence produced.

Mountain streams are known to have bed characteristics which vary in a predictable way as the stream is followed downstream (fig.43).



Figure 43:
Sequence of bed
characteristics of
mountain streams.

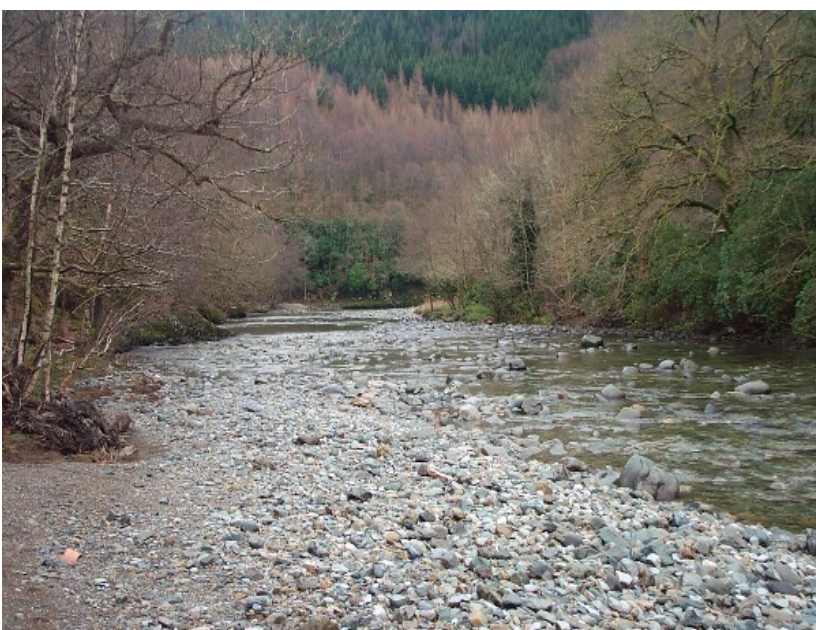
Cascade reach

Afon Ty Cerrig,
Pared yr Ychain.



Step pool reach

Afon Mynach,
Tai cynheaf.



Plane bed reach

Afon Mawddach,
Ty'n y Groes.

Close to the source, streams usually display a cascade structure with the bed largely covered by substantial blocks of rock. Downstream, the stream develops a step pool structure, with sections of rapids separated by pools of calmer water. Continuing downstream, the stream can develop a plane bed of gravel across the channel.

The changes in bed form are a response to increasing water flow and decreasing channel gradient as the stream descends from its mountain source. Linked to these changes are a downstream reduction in bed friction per unit width, and the amount of turbulence. These factors can be taken into account by water flow calculations for river routing.

Hillslope runoff model

Development begins by producing a topological model from digital elevation data on a 50m grid.

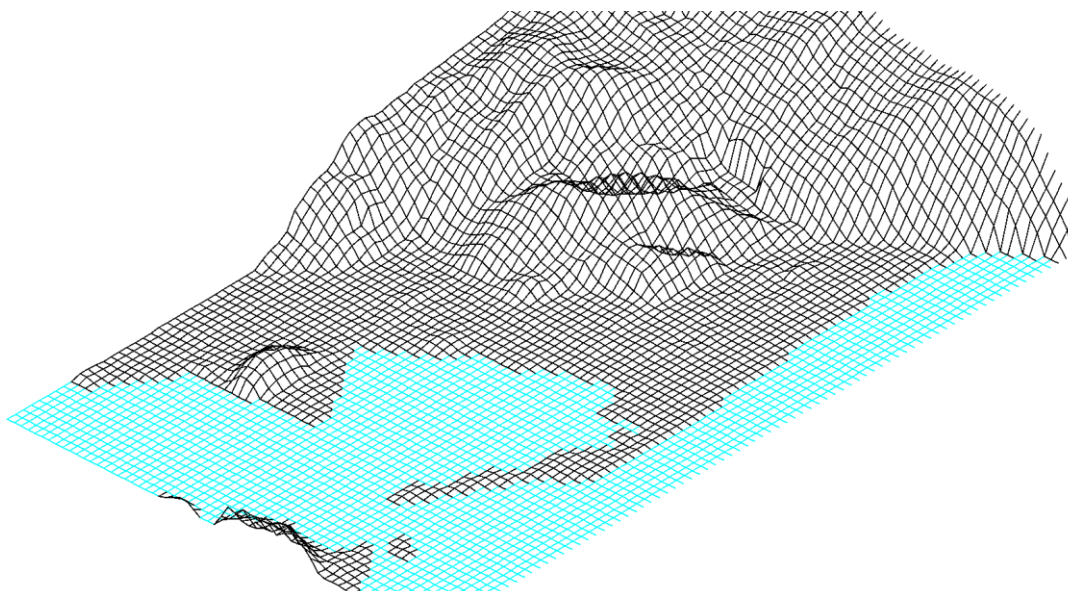


Figure 44:
Model for the catchments of the rivers Henddol and Morfa in the hills above Fairbourne.

The program then analyses the shapes of the hillslopes to determine the positions of streams.

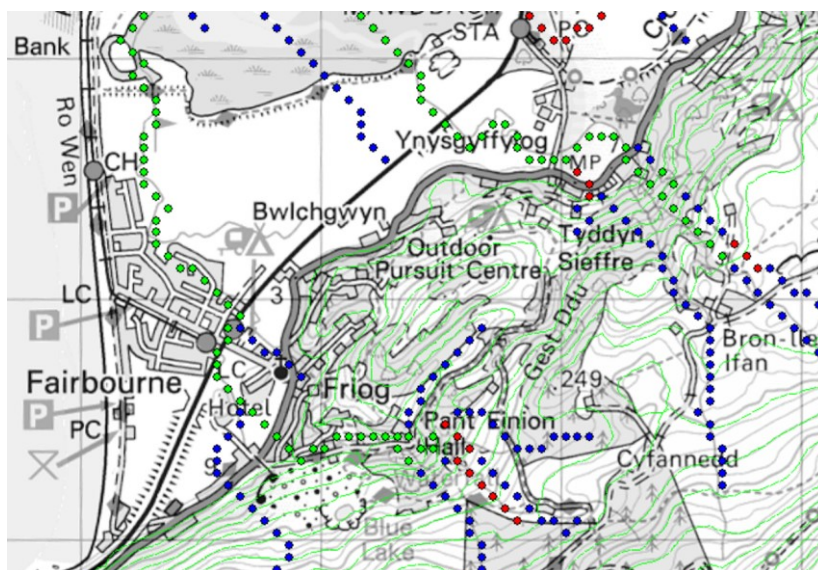


Figure 45:
Calculated locations of streams. These have been classified as: first order (blue), second order (red), or third order (green).

Streams have been classified according to their stream order. The system begins by designating all headwater reaches as first order. Where two first order streams meet, a second order stream is formed. Where two second order streams meet, a third order stream is formed, as in fig.46:

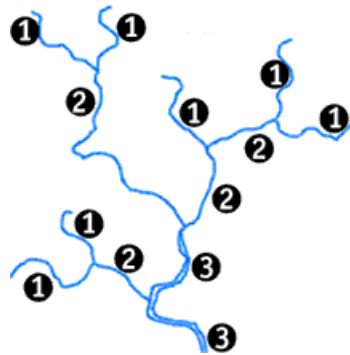


Figure 46:
System for allocating stream order numbers to branches of a stream network.

The allocation of stream order allows different values for turbulence and bed frictional resistance to be applied downstream through the stream network according to channel size.

The next stage in setting up the model is to predict the distribution of different soil types across the catchment areas of the rivers Henddol and Morfa, so that flood runoff can be estimated. In addition to wetness index and geology, the HOST soil class can be affected by vegetation. Soils are found to be deeper below woodlands than below grassland, due to increased incorporation of organic material from leaf and needle fall and greater trapping of soil particles washed down the hillslope.

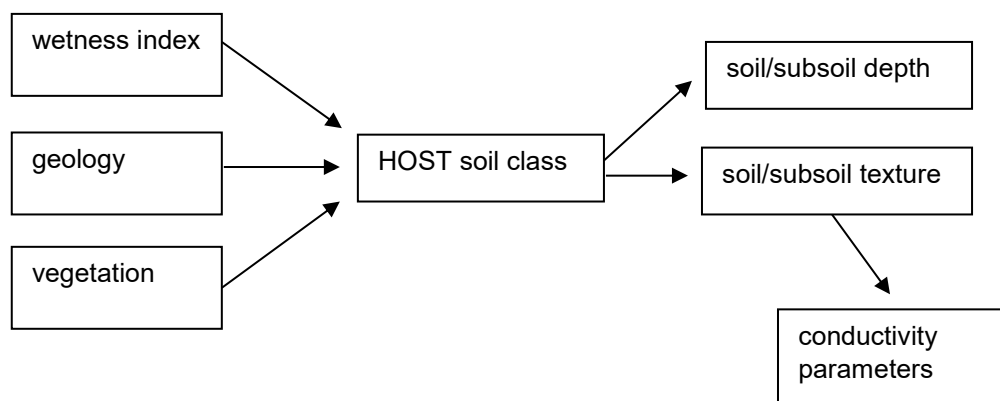


Figure 47: Stages in the determination of soil parameters for the hillslope model.

Once the HOST soil class has been found, the soil and subsoil depth can be estimated, along with the porosity and hydraulic conductivity of the soil and subsoil.

Calculations to determine HOST soil class are based on digitised maps of geology and land use, prepared using a geographical information system (fig.48).

The final stage in setting up the model is to specify the input rainfall sequence for the hillslope runoff simulation. A four day period in February 2004 has been chosen, when a series of closely grouped weather fronts caused near continuous intense rainfall across Snowdonia (fig.49). This led to serious flooding in Dolgellau and other towns, and the railway at Betws y Coed was washed away by flood water. This event probably represents a worst case river flood scenario for Fairbourne.

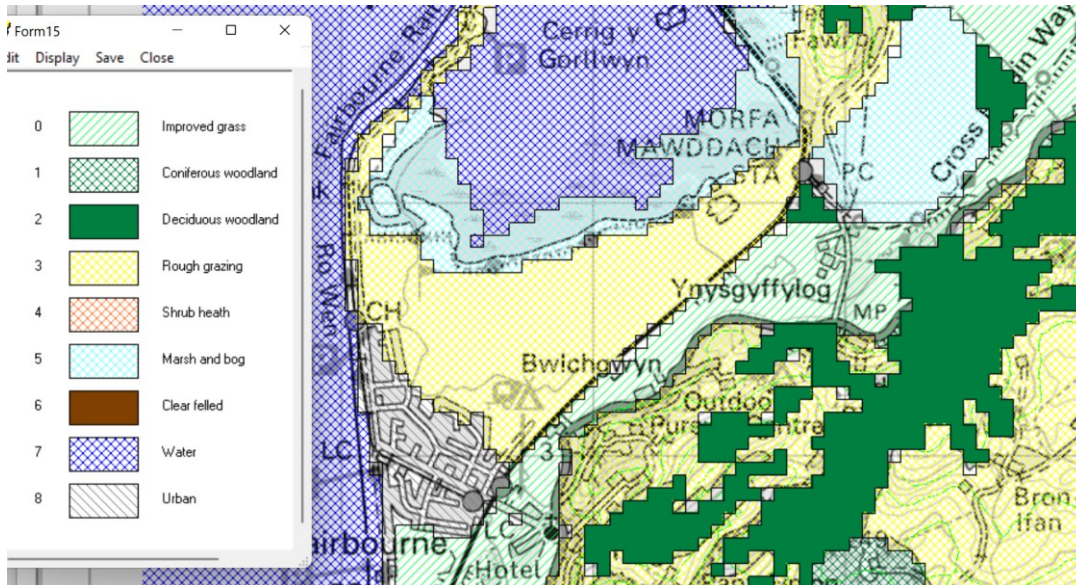


Figure 48:

Map data for determination of soil class:

(above) vegetation

(below) geology

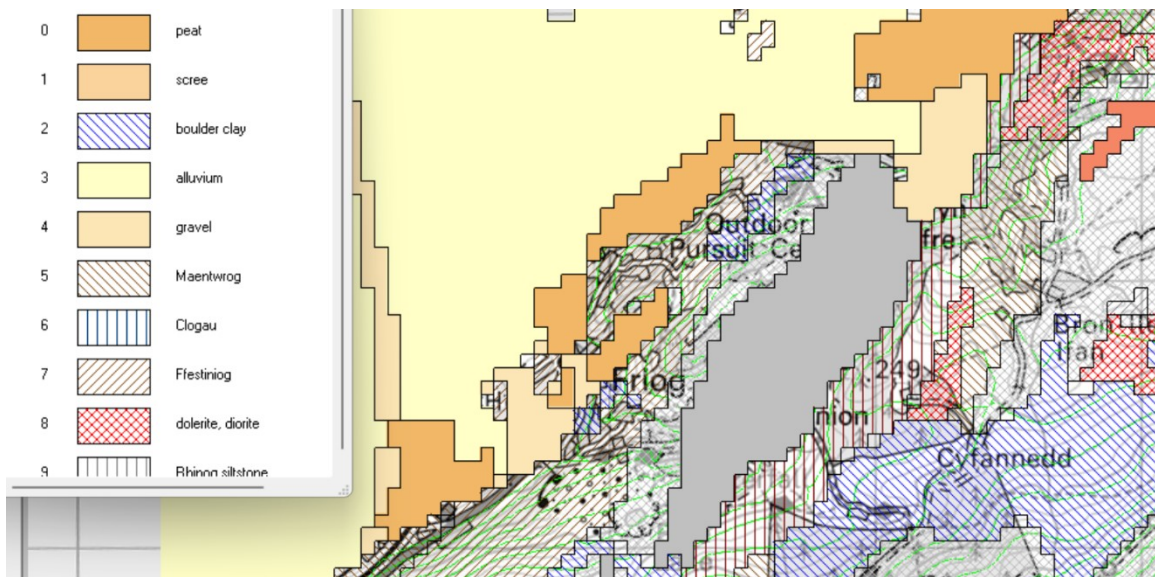


Figure 49: Hourly rainfall sequence for the February 2004 storm event.

The simulation was carried out for the duration of the four day storm event. The output displays the level of soil saturation, with green and yellow indicating a water table near the surface. Red colour represents an open stream channel or surface water flooding.

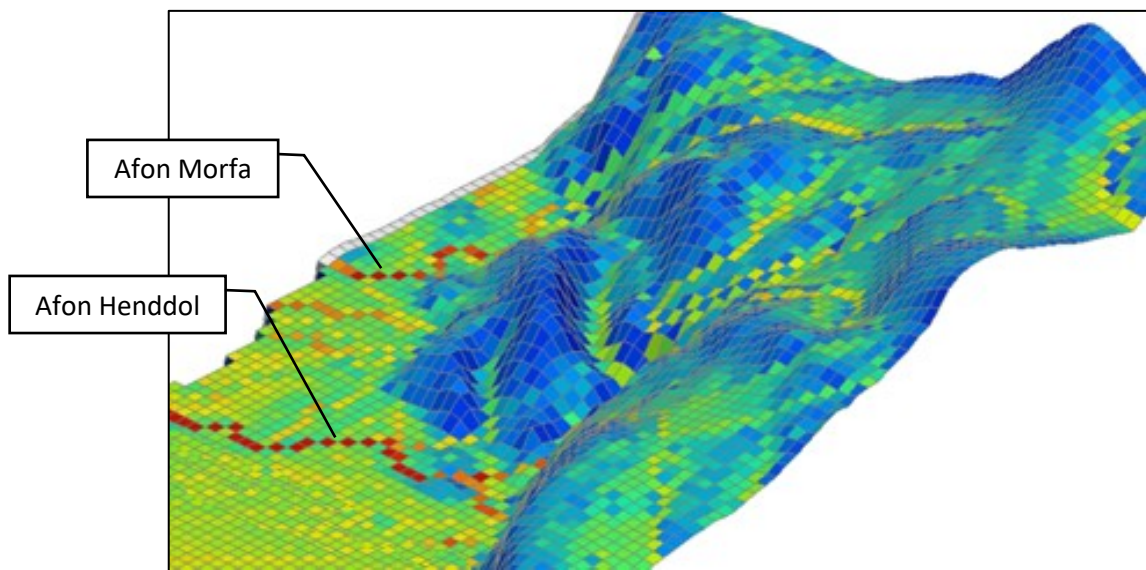
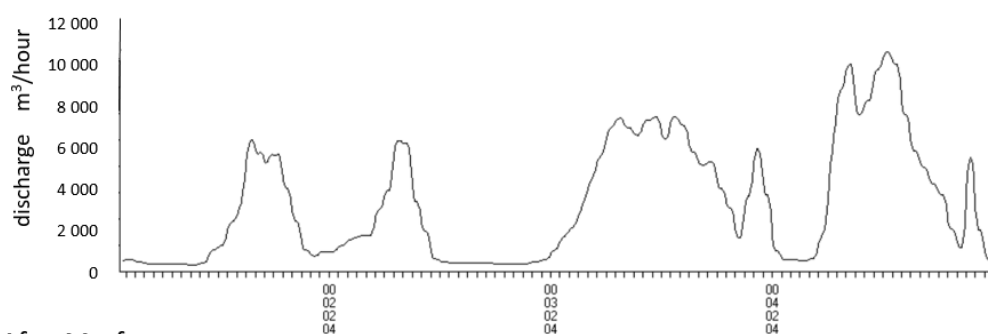


Figure 50: Hillslope runoff model for the Henddol and Morfa catchments.

Hydrographs were obtained for the Afon Henddol and the Afon Morfa at the points at which they pass through culverts beneath the railway embankment to the east of Fairbourne. These will be used as input to a coastal lowland flood model for the Fairbourne area.

Both hydrographs show similar patterns, with the maximum discharge from the Afon Henddol slightly larger due to a catchment area of 3.5 km² in comparison to 3.2 km² for the Afon Morfa. For both rivers, the runoff progressively increases during the four days of the storm event. This is due to increasing saturation of the soil and subsoil, so that rainfall interception decreases and the amount of fast overland flow into streams increases.

Afon Henddol



Afon Morfa

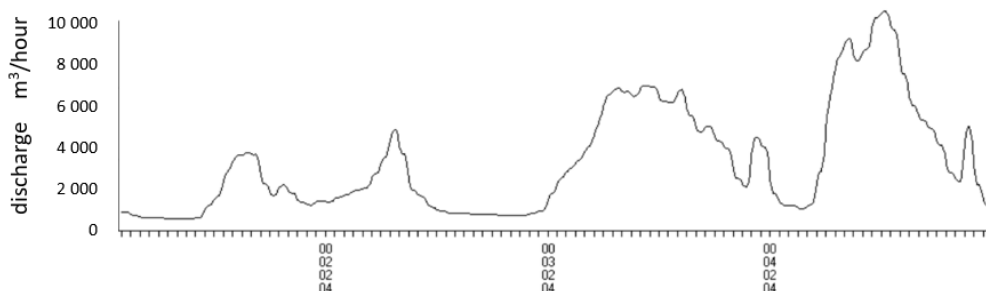


Figure 51:
Modelled hydrographs for the February 2004 storm event

5. MARINE SYSTEM

It has been suggested that there is a serious and increasing risk of failure of the sea defences at Fairbourne, leading to sudden catastrophic flooding of the village. This claim will be examined.

As a separate issue, sea water may wash over the sea wall due to wave action during storms. The risk of surface water flooding in the village will be evaluated by estimating the volume of wave overtopping during a worst case storm event. A further concern would be erosion of the surface of the landward side of the coastal embankment by overtopping waves.

Coastal erosion processes at Fairbourne have been examined in detail by Phillips, Thomas, and Morgan (2017). They identified erosion taking place at the end of the shingle spit at Friog cliff. This erosion had led to the failure of the sea wall in a storm during 2014, with localised flooding of the nearby mobile home park. A contributing factor in the sea wall failure seems to have been the removal of shingle from the landward slope of the pebble embankment to create a flat area in front of huts at this location. It is recommended that this material is replaced to strengthen the sea wall structure.



Figure 52: Coastal defences at Friog.

The sea wall was rebuilt by Natural Resources Wales and rock armour added (fig.53). The new structure has provided good protection during subsequent storms, and there is no current risk to this section of the shoreline. In the longer term, up to and beyond the year 2065, the risk of catastrophic failure of the sea wall at Friog now appears to be low. In the unlikely event of failure, the resulting flooding would be localised and would not be a threat to the village.



Figure 53:
Coastal defences at Friog after repair of the sea wall and addition of rock armour.

Coastal erosion is, however, continuing at Friog. Future flood risk could be reduced by construction of an offshore reef of boulders, similar to the structures added to the beach at Borth (fig.54). This would cause waves to break on the lower sandy beach, and sediment would accumulate in the sheltered water in front of the current shingle storm beach.



Figure 54: Boulder reefs providing coastal defences at Borth.

Surveying carried out over a number of years (Phillips, Thomas, and Morgan, 2017) indicates that the shingle storm beach in front of Fairbourne village is stable (fig.55), whilst the storm beach to the north of the village is slightly increasing in volume.



Figure 55: View northwards towards Fairbourne, showing the very substantial shingle storm beach.

Some beach material may be lost due to erosional wave action during storms, when waves break higher on the shingle bank and backwash carries shingle towards the sea. However, this material is normally replaced over the following months by constructive wave action (fig.56), when waves break lower on the beach and the swash moves shingle back up the storm beach.

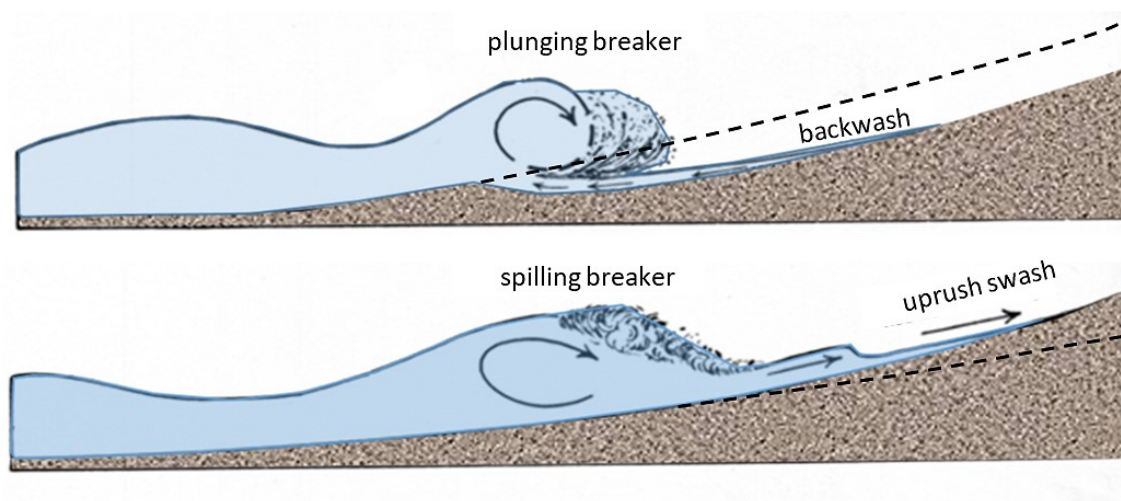


Figure 56: (above) erosional wave action (below) constructive wave action.

It can be concluded that the storm beach and embankment in front of Fairbourne village is stable and extremely substantial, so the risk of catastrophic failure is negligible.

Wave overtopping

The problem of wave overtopping during storms will now be considered. An objective is to estimate the volume of water which could be transferred across the sea wall by wave action during a worst case storm as predicted for the year 2065.

Wave data was compiled for a point approximately 5km off-shore from Llwyngwriil, south of Fairbourne, for the period 1980-2016 (Phillips, Thomas, and Morgan, 2017). This is shown in fig.57.

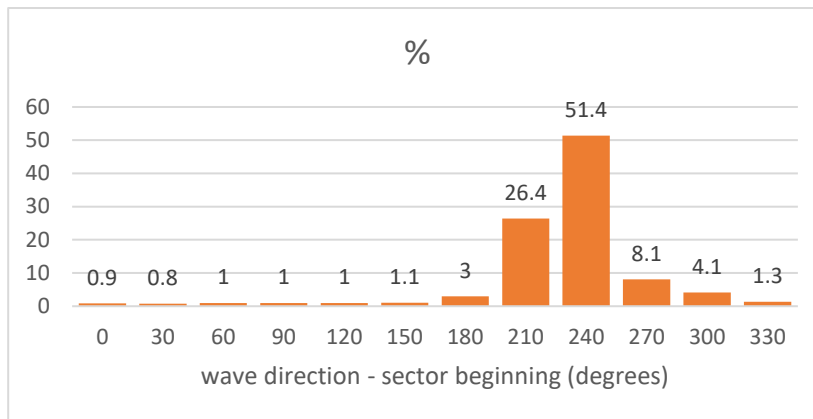
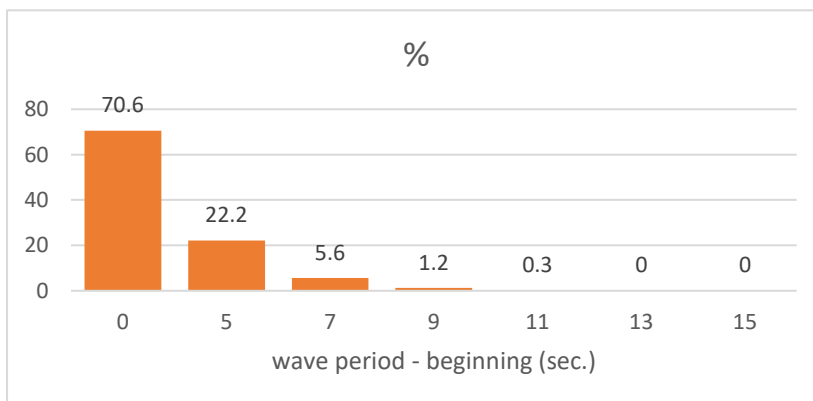


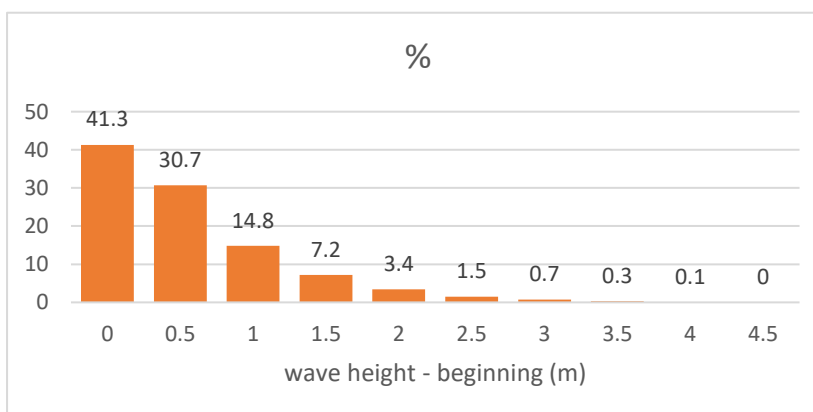
Figure 57:

Wave data collected off-shore from Llwyngwriil for the period 1980-2016.

A majority of waves originate from the south west, between compass bearings 210° and 270°.



Most waves have a period between 0 and 5 seconds, with a maximum recorded wave period of between 11 and 13 seconds.



Most waves have a height of less than 1.0m. The highest waves recorded were between 4.0 and 4.5m.

The wave period is the time required for one complete wave length to pass a fixed point, usually measured between two successive wave crests. Wave period is of importance as it is linked to the amount of kinetic energy carried by the wave swell. Wind blowing across the sea produces waves. The stronger the winds and the longer their duration, the more energy will be transferred to the water and the deeper this energy will penetrate below the sea surface.

When waves move across the sea, there is no actual flow of water from place to place. Instead the water moves in orbits beneath the surface, creating a wave trough as it moves downwards and a crest as it moves back upwards (fig.58).

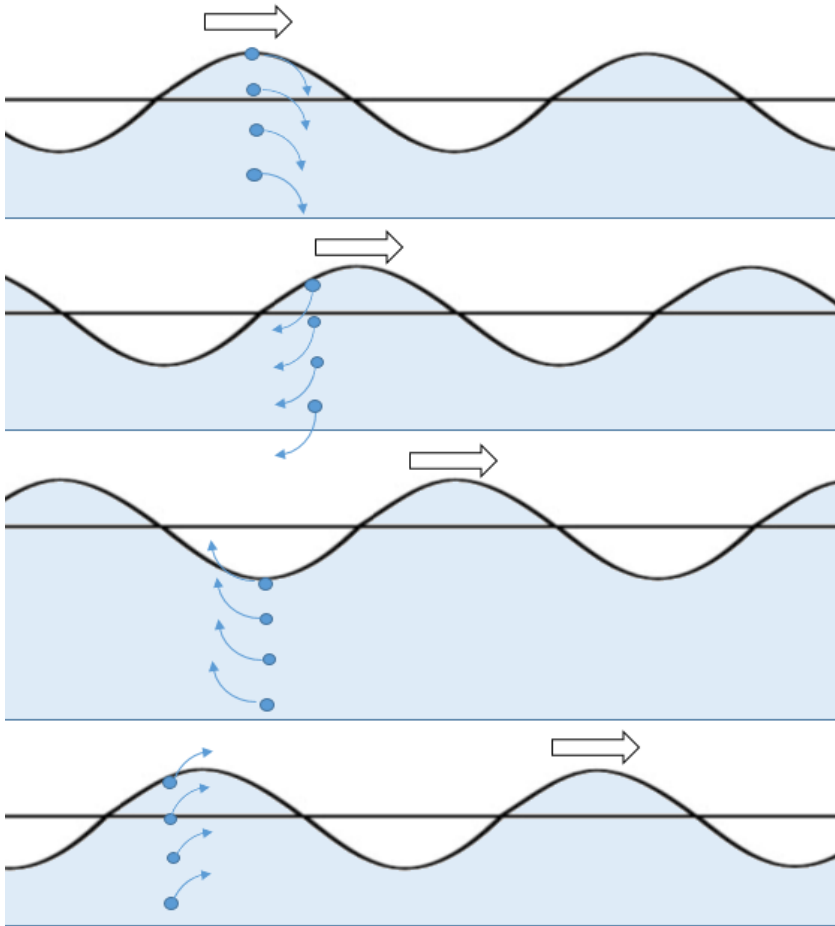


Figure 58:

Wave transmission by circular motion of the underlying body of water.

A longer-period wave has larger orbits of underlying water which extend to a greater depth below the surface before the motion dies out. In this way, a long period swell carries a larger amount of wave energy. On approaching a coast, a long period swell can make contact with the sea bed earlier, which causes waves to overturn and break further from the shore on a gently shelving beach.

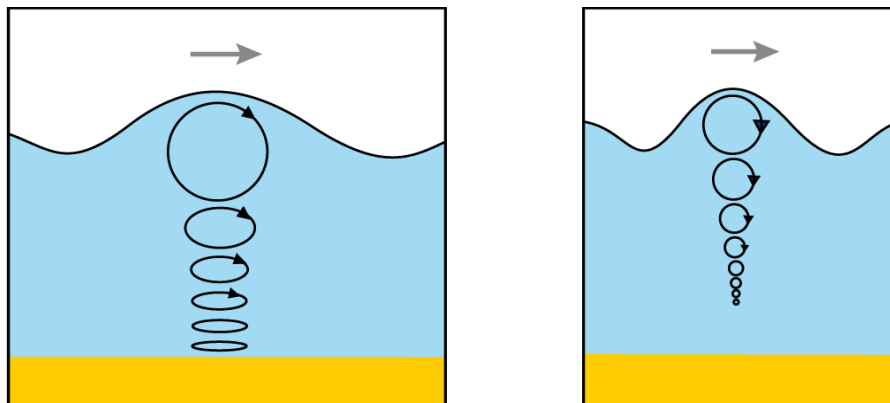


Figure 59: Water motion beneath long and short wavelength swells.

Current wave action at Fairbourne has been modelled by Phillips, Thomas, and Morgan (2017), and verified by wave observations during storms. It was found that offshore extreme waves can reach a height of 5.9m above astronomical tidal level, with an associated period of 10.5 seconds. These extreme storm conditions would be expected once in 100 years.

To the south of Fairbourne village, waves maintain most of their height until around 900m from the shingle bank, where sea bed depth is sufficiently shallow to influence the wave motion. There is a substantial reduction in height, then around 200m from the shore, the wave breaks and runs up onto the shingle bank (fig.60).

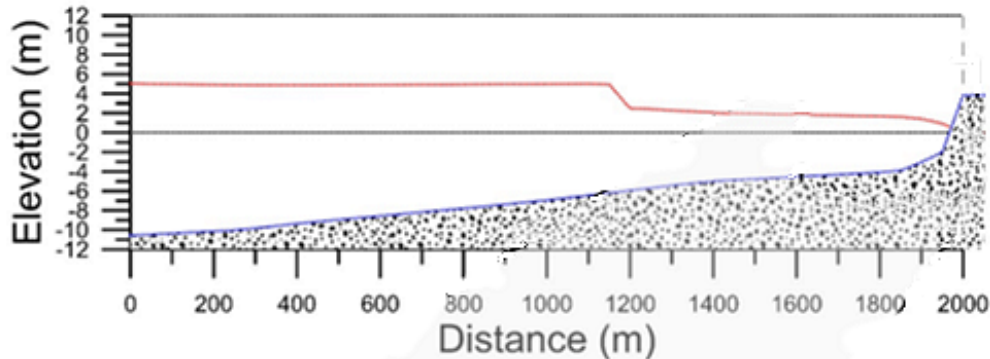


Figure 59: Wave modelling by Phillips, Thomas, and Morgan (2017) for an extreme storm with an offshore wave height of 5.9m above astronomical tide height. Wave height reduces to less than 1m by the time that the shingle bank at Fairbourne is reached.

Further along the shore in front of Fairbourne village, the waves start to break slightly further offshore at around 1100m from the shingle bank.

The modelling by Phillips, Thomas, and Morgan did not identify any wave overtopping of the shingle bank around Fairbourne village under extreme storm conditions for current sea level, storm surge and wave heights.

Further investigations for the current study were carried out using EUROTOP software. This was developed in the Netherlands for the safety assessment of coastal defences. The program is intended to model wave action at dykes and embankment structures with a sloping seaward face. Roughness and permeability of the embankment materials are taken into account, making the model suitable for investigating the Fairbourne shingle storm beach and sea wall.

The input parameters required by the program are: the still water level at the embankment; the angle of wave approach to the shore line; a representative wave period; the wave height at the embankment; and the storm duration. It is also necessary to enter the geometric profile of the embankment, along with details of its constituent materials.

During a storm, there are likely to be waves breaking on the shore with a variety of different periods. The longer waves carry the most kinetic energy, so are most likely to overtop the embankment. The software uses a value called the *spectral wave period* in its calculations. This represents the wave period for high energy but relatively common waves observed during a storm. It is about 90% of the maximum wave period observed.

Calculations depend also on the heights of the waves during the storm. It is found that a typical distribution of wave heights is heavily skewed (fig.60). If the numerically most common wave height is found, relatively few waves are lower than this, but higher waves occur quite frequently. It is, of course, these higher waves which are most likely to overtop the embankment. The wave height used by the program for its calculations is therefore the *significant wave height*, which is defined as the average height of the highest one-third of all waves.

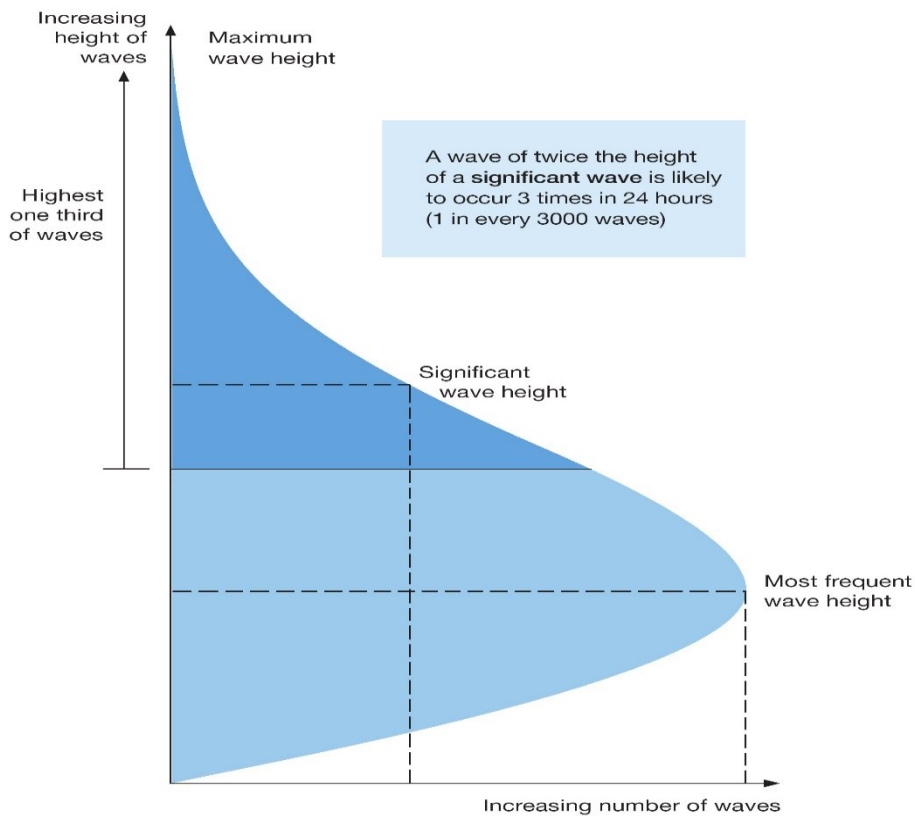


Figure 60:
Spectrum of wave heights experienced during a typical storm.

Waves approaching Friog are parallel to the shore but further along the coast at Fairbourne, waves approach at a slight angle of 10° to the shoreline (fig.61).

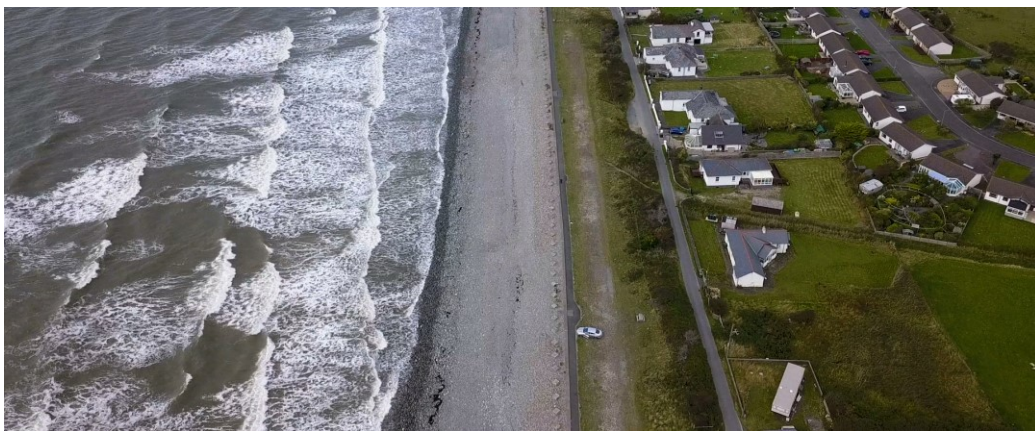


Figure 61: Approach angle of waves at Fairbourne village.

The software carries out a statistical simulation of a sequence of waves approaching during the storm. The program determines the energy of each wave from its swell period, which in turn predicts its behaviour on contacting the shoreline. The likelihood of wave overtopping varies according to whether the wave plunges or spills onto the storm beach.

The height reached by the highest 2% of incoming waves is determined. This point is measured vertically with respect to the still waterline.

The program calculates how much water passes the seaward crest of the embankment and is assumed to overtop the structure. In practice, some or all of this water may be dissipated into the permeable shingle of the embankment's upper surface, especially where this is wide. The calculated result is therefore a worst case. The percentage of the waves that reach the seaward crest is also shown. Results of the analysis are given in fig.62 below.

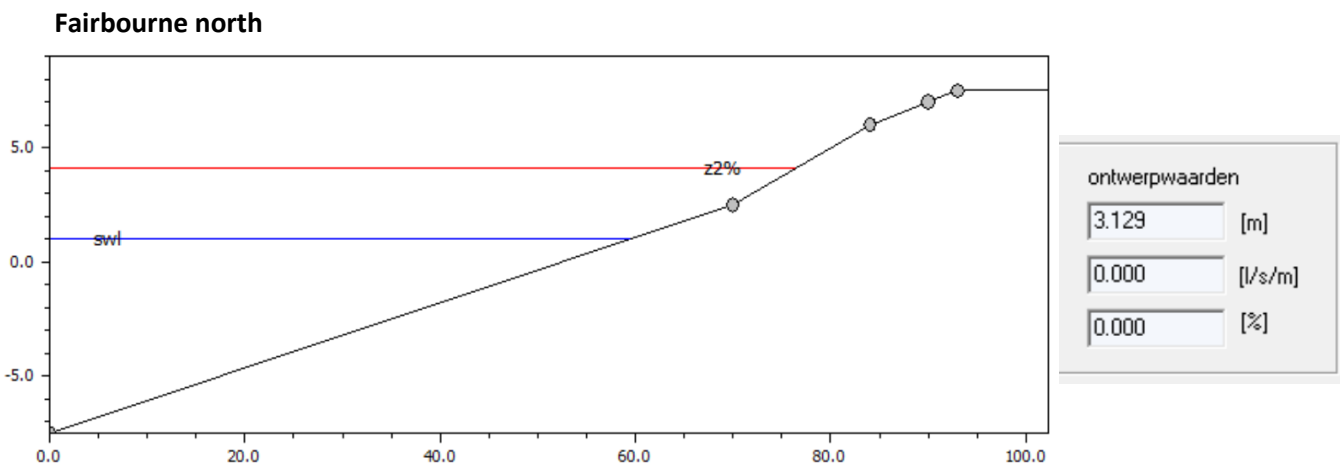
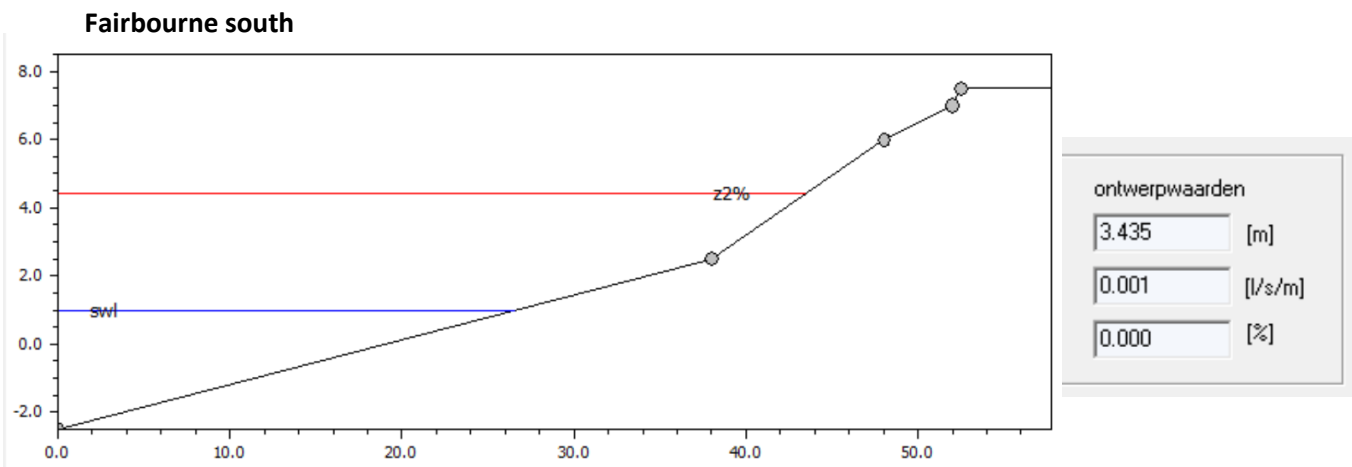
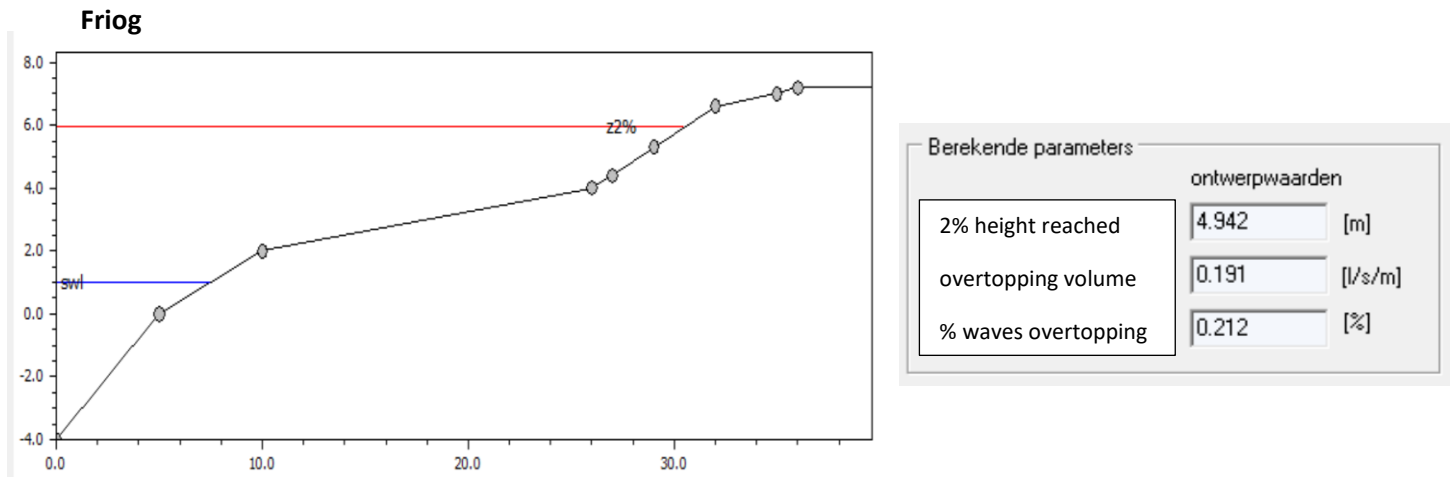


Figure 62: Modelling to determine wave overtopping volumes for a worst case storm based on sea level prediction for 2065.

Results indicate that wave overtopping is restricted mainly to the storm beach to the south of Fairbourne, with a negligible amount of sea water crossing the embankment in front of Fairbourne village.

Wave overtopping is only likely to occur within one hour either side of a high spring tide combined with an exceptional storm surge. The amount of overtopping rapidly reduces northwards away from Friog. Taking these factors into account, a reasonable upper limit for wave overtopping during a worst case storm is 8,000 m³. This represents an addition to the Fairbourne internal drainage system of 2 m³/second at peak flow. For the purpose of the current project, the wave overtopping discharge will be modelled as increasing linearly from 0 to 2 m³/second in the hour up to high tide, then decreasing linearly to 0 in the hour after high tide.

Some concern must remain that the overtopping waves between Friog and Fairbourne could erode the landward side of the embankment, weakening the structure:

- One solution is to raise the height of this section of the storm beach and sea wall by 1m.
- An alternative would be to provide a protective surface covering of shingle on the landward side of the embankment, to absorb overtopping water and transfer it to a buried drain (fig.63). Shingle should be positioned at a rest angle of less than 30° to ensure that the slope is gravitationally stable.

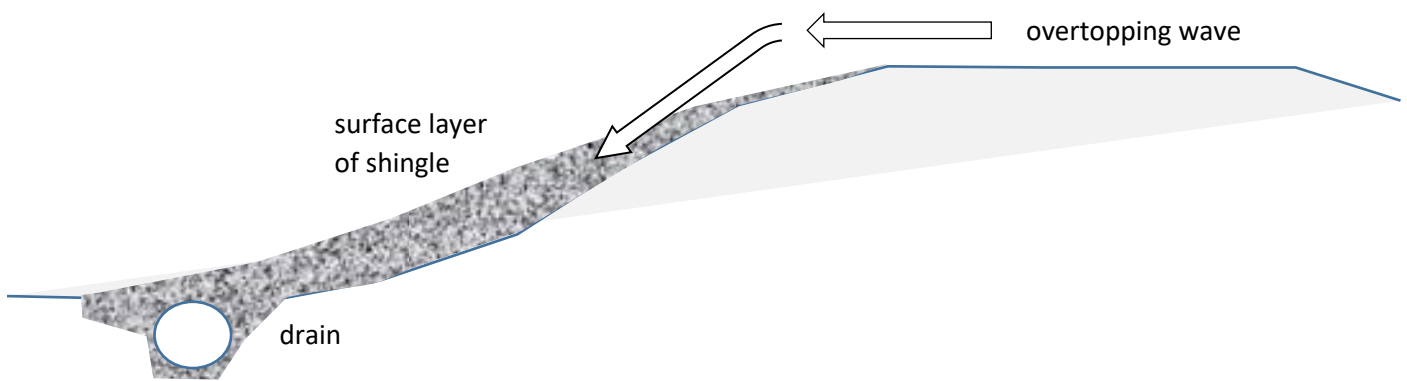


Figure 63: Addition of shingle to the landward face of the sea embankment to facilitate drainage and prevent surface water damage.

Sufficient space is generally available alongside the road for this work to be carried out if it is found to be necessary (fig.64).



Figure 64: Landward face of the sea embankment to the south of Fairbourne village.

6. COASTAL LOWLAND SYSTEM

The coastal lowland between Fairbourne and Arthog lies within the current flood defence area. It is protected from estuary flooding by a chain of embankments which were rebuilt and strengthened during the 2016 flood alleviation scheme.

The present day geological structure and landscape of the coastal plain is the result of events which occurred during and after the Ice Age. In the late stages of ice retreat, around 12,000 years ago, sea level was approximately 30 metres lower than at the present day. A major glacier which had occupied the lower Mawddach valley was now retreating, leaving extensive moraine deposits in Barmouth Bay (fig.65). The River Mawddach carried a mixed sediment load produced during the melting of mountain and valley glaciers. Coarser gravels were deposited at the head of the present estuary as the river gradient was reduced. Finer material was carried downstream, with sands deposited in the active river channel and mud deposited on the floodplains. The Mawddach discharged westwards into the sea via channels through the moraine ridges, and northwards through coastal lagoons.

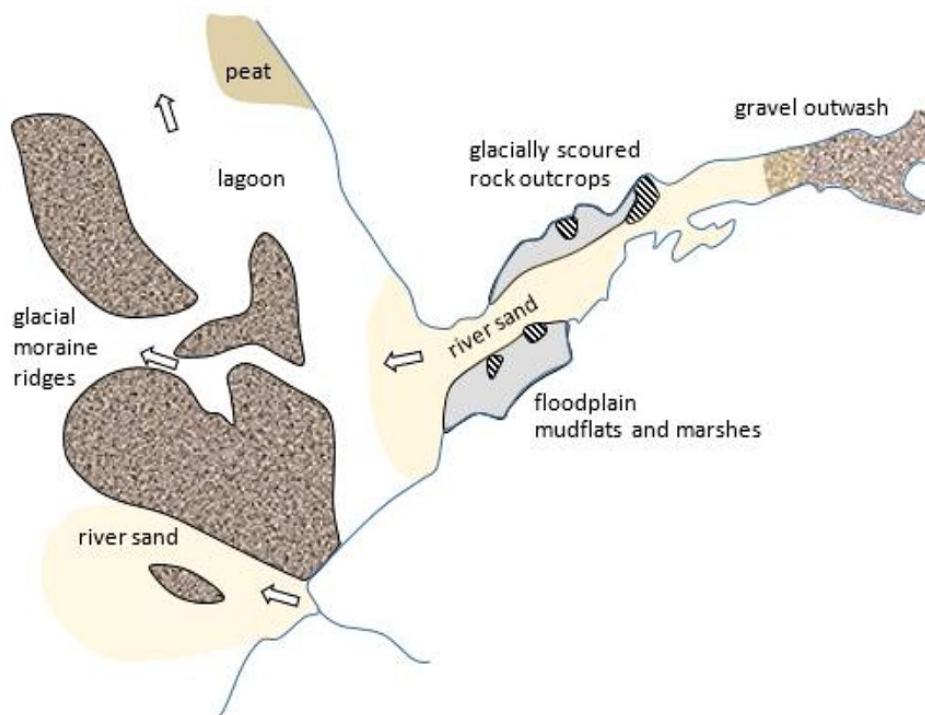


Figure 65: Sedimentation around the Mawddach estuary in the Late Devensian stage of ice retreat, 12,000 years before the present (Larcombe & Jago, 1994).

By about 6,000 years before the present, sea level was at about the same level as the present day. The moraine ridges off the mouth of the Mawddach had become submerged, and the estuary was now tidal. Growth of a shingle spit had begun, fed by the longshore drift of pebbles from coastal deposits around Llwyngwrl (fig.66).

Sea bed erosion in Barmouth Bay provided sand which could be carried into the estuary on inflowing tides. Extensive deposition of marine sand occurred in the glacially over-deepened lower estuary, including the bays to the west and east of the Arthog coastal plain.

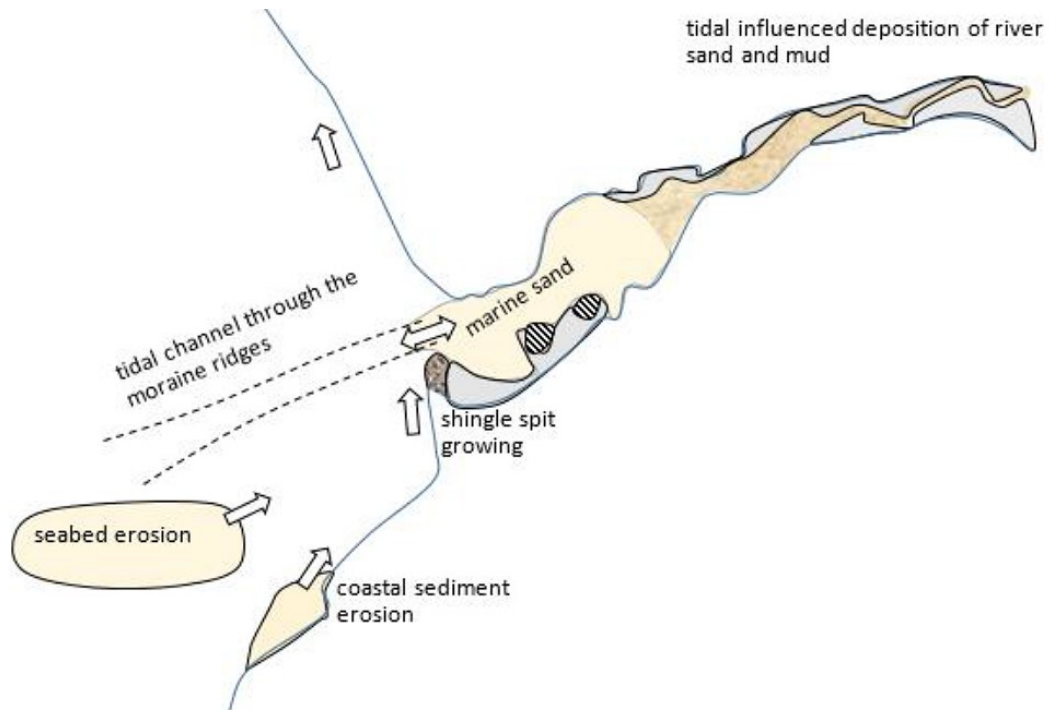


Figure 66: Sedimentation around the Mawddach estuary after ice retreat, 6,000 years before the present (Larcombe & Jago, 1994).

At the present day, we see rocky outcrops on the coastal plain, surrounded by flat land underlain by deposits of sand, clay and peat (fig.67). There is a very slight gradient towards the estuary, allowing rivers to drain to tidal gates in the estuary embankments.



Figure 67: View from Morfa Mawddach across the coastal lowland towards Fairbourne. A former rocky island emerges through estuarine deposits of sand and clay.

A geological map of the coastal lowland is given in fig.68. Estuarine sands and clays form most of the flat land underlying Fairbourne village and the surrounding agricultural land. Peat and gravel deposits are found to the south, along the edge of the valley.

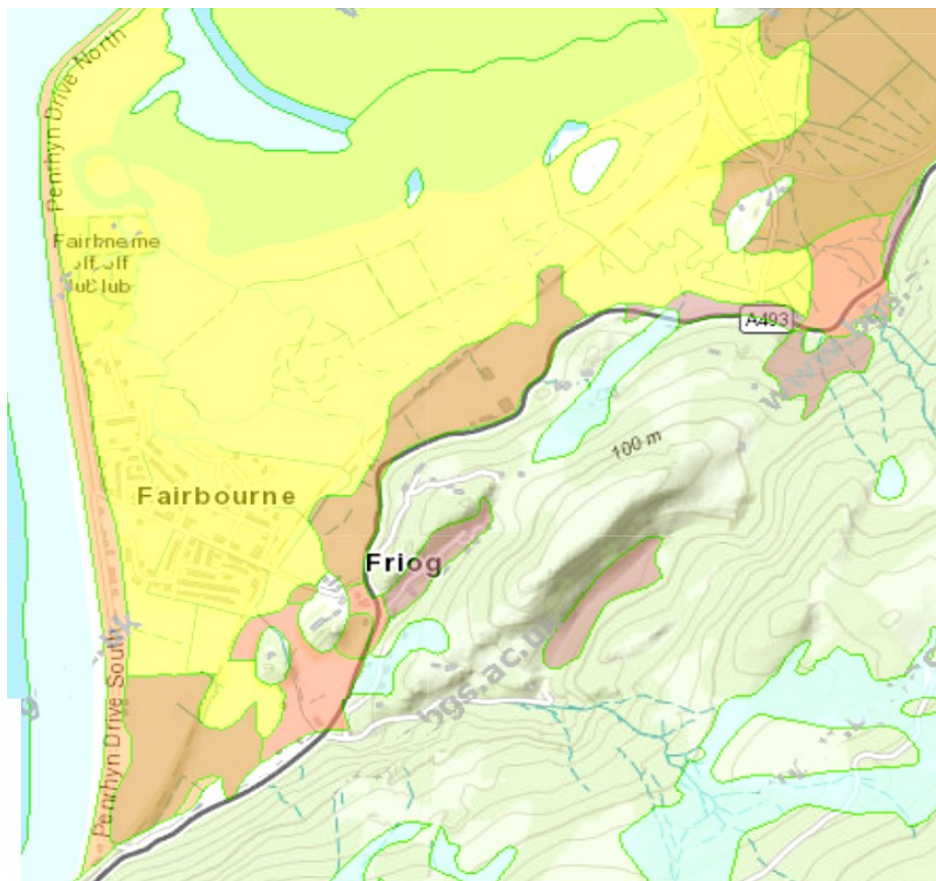


Figure 68:

Superficial deposits of the coastal lowland.

-  estuarine sand, clay
-  peat
-  glacial outwash sand and gravel
-  boulder clay

The underlying superficial deposits strongly influence the development of soils, which in turn affect the flood response of the area during storms. The more peaty soils tend to be heavier and wetter, as at Ynysgyffyllog (fig.69).



Figure 69: Soil profile at Ynysgyffyllog. This consists of a mixture of highly decomposed humified peat with alluvial sediment. The sand content is greater in the upper 60cm, with clay dominating below this.

In the coastal lowland nearer to the mouth of the estuary, soils are usually derived from estuarine deposits with alternating layers of sand and clay, as in fig.70.



Figure 70: Soil profile on agricultural land to the east of Fairbourne golf course. A layer of orange sand overlies grey clay (photograph by Owen, 2010).

Groundwater levels in and around Fairbourne village have been monitored by Buss (2018). Typical measurements, obtained at two locations in the village, are shown in figure 71.

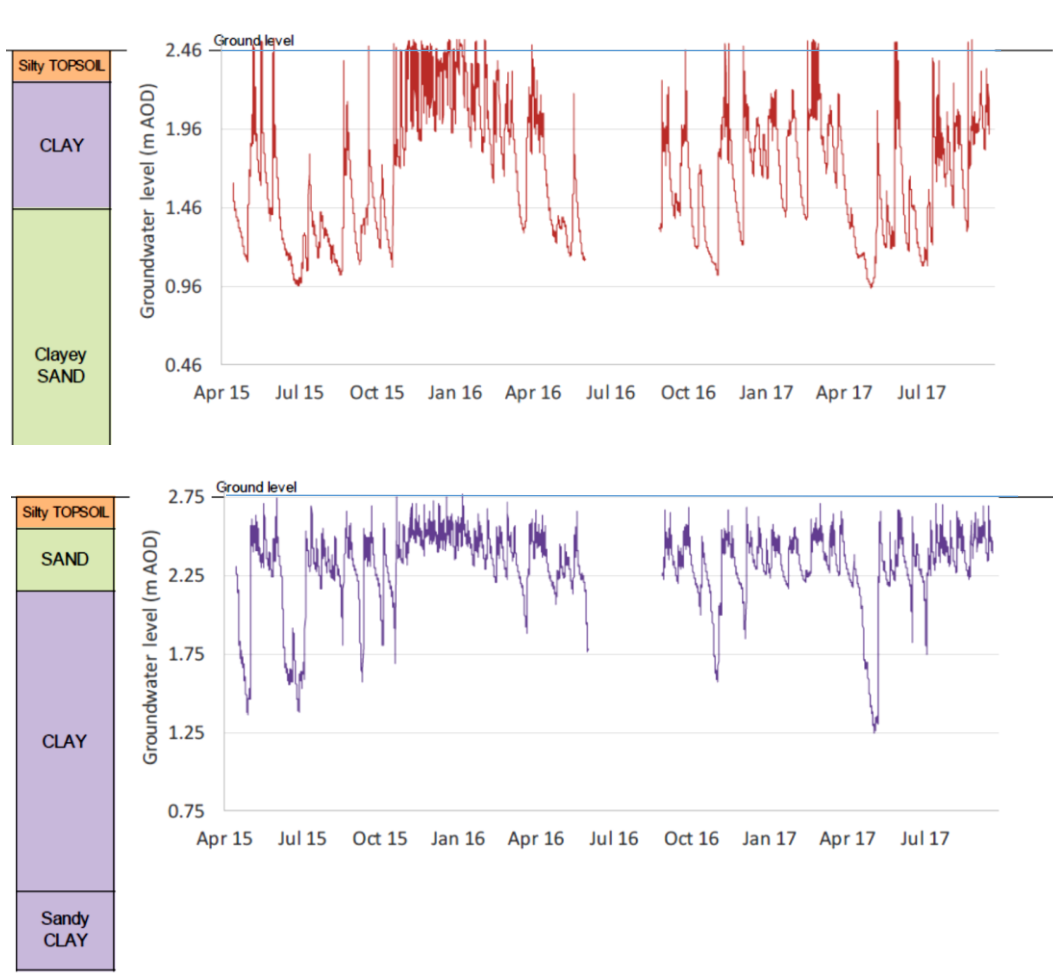


Figure 71: Groundwater levels recorded at two locations in Fairbourne village (Buss, 2018).

Both locations show a variation of about 1.5m in the depth of the water table, presumably in response to periods of rainfall and dry weather. Soil at the first location, where the upper layer consists of clay, appears to remain saturated for longer periods than soil at the second location where the upper layer is sand. However, both sites are generally well drained.

Interesting features of both graphs are short timescale variations in groundwater depth, which appear to be linked to tidal flows. Varying hydrostatic pressures caused by rising and falling tides cause movement of groundwater through permeable layers of sediment beneath the coastal lowland, particularly within areas of sandy subsoil. This process has been further investigated in the study by Buss. It is found that changes in tidal water level can be transmitted through the shingle storm beach, affecting the groundwater level beneath the village (fig.72). The variation in the water table depth is, however, much less than the tidal range. A tidal range of 5m between low and high water produces a groundwater variation of only 50cm below the village.

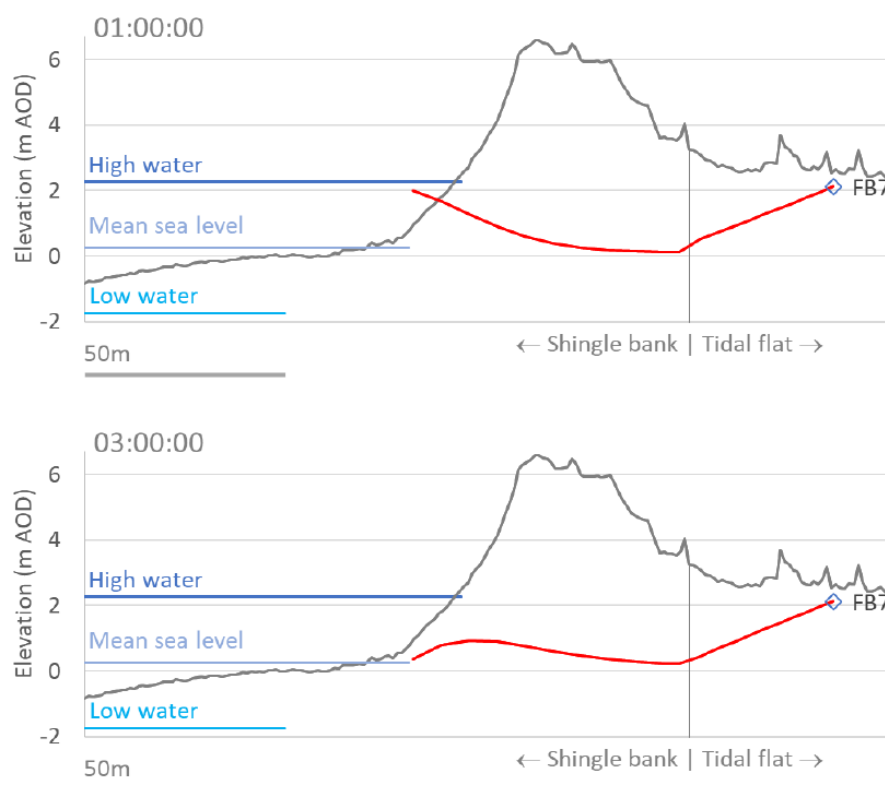


Figure 72: Variations in groundwater level beneath the Fairbourne shingle embankment in response to tidal height (Buss, 2018).

Further examination of the groundwater profile showed that the water table is depressed close to a drainage ditch (fig.73) as water flows out towards the estuary tidal gate where it is discharged at low tide.

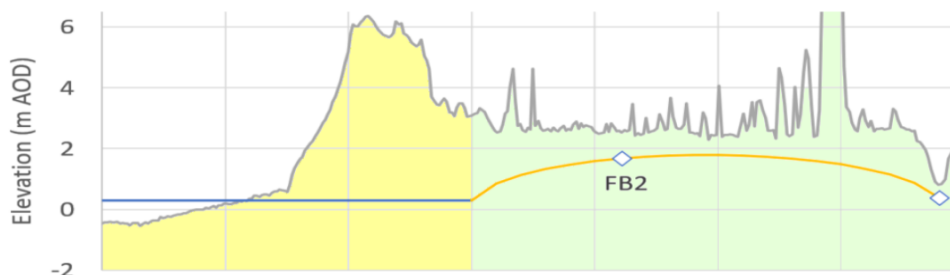


Figure 73: Variation in groundwater level beneath Fairbourne village.

Two small rivers cross the coastal lowland:

The Afon Henddol flows across fields to reach Fairbourne (fig.74), then skirts around the village before continuing northwards to the estuary tidal gate near the golf course.



Figure 74: Afon Henddol flowing towards Fairbourne village (photograph by Owen, 2010).

Under the proposed flood protection scheme, the Afon Henddol would be re-routed eastwards, then enter the estuary through a tidal gate shared with the Afon Morfa. The former tidal gate of the Afon Henddol would remain in use, but only for drainage from within the Fairbourne village flood protection boundary.

The Afon Morfa descends from the hillside above Ynysgyfflog, then crosses the coastal lowland (fig.75) to reach its tidal gate and discharge into the estuary (fig.76).



Figure 75: Afon Morfa flowing from the hills above Ynysgyfflog.



Figure 76:

(above) Tidal gate outfall of the Afon Morfa.

(below) Channel from the Afon Morfa outfall crossing tidal flats of the Mawddach estuary.



It will be necessary to increase the discharge capacity of the Afon Morfa tidal gate to handle the larger combined outflow from the two rivers. Alternatively, a new tidal gate for the re-routed Afon Henddol could be built through the estuary embankment nearby.

Hydrological model

A model was constructed to determine whether the proposed flood protection scheme for Fairbourne would be able to safely handle storm water discharge. A worst case storm event was modelled, based on climate change predictions for the year 2065.

The model was developed as a modified version of the Mawddach hillslope model, used earlier in section 4 to determine peak flows for the rivers Henddol and Morfa. Functions were added to allow the accurate representation of the sea wall, railway and other embankments, and the rivers and drainage ditch network. Hydrological functions simulate the operation of the tidal gates and a flood water retention pond which will be located to the east of Fairbourne railway station.

The model is based on a 50m digital elevation grid for the coastal lowland between Fairbourne and Ynysgyfflog, as shown in fig.77 below.

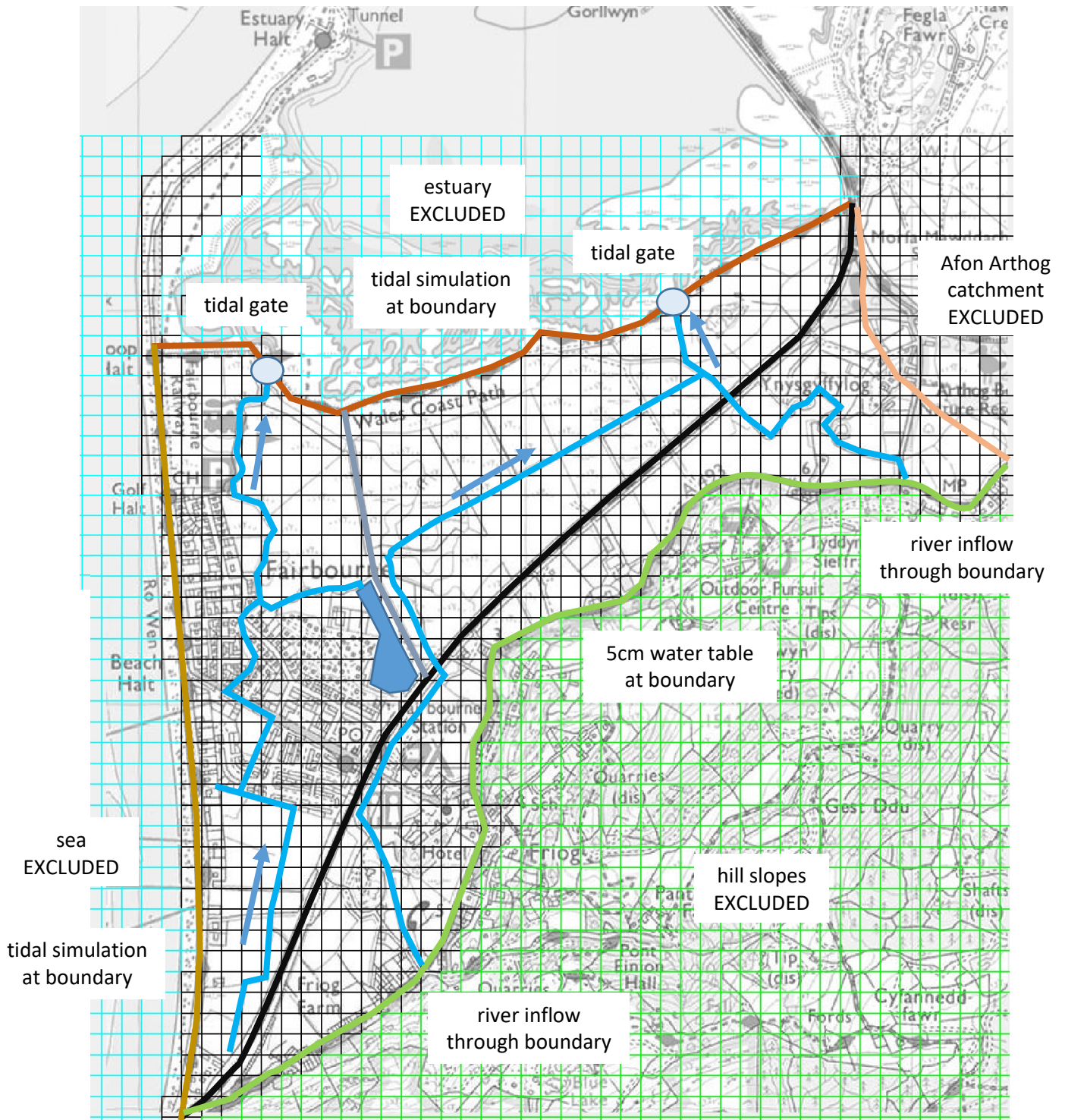


Figure 77: Structure of the coastal lowland model.

The hill slopes to the south of the coastal lowland are excluded from the model. The soil at the base of the slope is assumed to be constantly saturated up to 5cm from the surface, consistent with the hillslope storm runoff results obtained in section 4 above. Shallow throughflow of water into cells of the coastal lowland model may occur along this boundary.

A very low watershed occurs at Ynysgyfflog, with water flowing either westwards towards the Afon Morfa tidal gate, or eastwards to the Afon Arthog tidal gate. The area of the Afon Arthog catchment to the east is excluded from the model. It is assumed that no movement of water takes place across the watershed boundary.

The railway embankment and the proposed embankment to the east of Fairbourne village are assumed to be impermeable above ground level, but may allow movement of ground water beneath the structure in response to a difference in hydraulic head. The rate of flow will be determined by the hydraulic conductivity of the soil and subsoil.

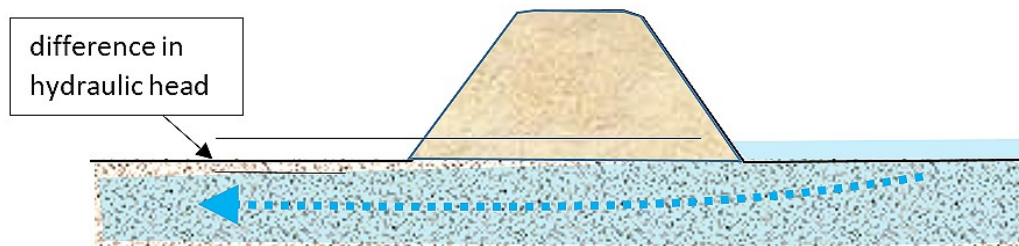


Figure 78: Modelling of possible water flow beneath embankments.

The sea embankment and estuary embankment are similarly assumed to be impermeable above ground level for all tidal heights. There is no evidence of seepage through either structure at high tide at the present day, and modelling indicates that no direct overflow of either structure will occur under the most extreme storm conditions predicted for the year 2065.

Water table monitoring by Buss (2018) has found that movement of groundwater beneath the shingle spit is possible in response to tidal flows. Sea and estuary water may move into the subsoil below the coastal lowland when the tidal height is above the level of the land. Conversely, groundwater may move outwards towards the sea or estuary when the tidal level is lower than the land. The model simulates tidal cycles, and allows for groundwater movements according to the hydraulic conductivity of the soil and subsoil, and the differences in hydraulic head caused by changes in the tidal height.

The objective of the model is to assess the response of the Fairbourne internal drainage ditch system, tidal gate and flood water retention pond during a worst case storm event. Rainfall is applied for the same period of four days of extreme frontal rainfall which was simulated in the hillslope runoff model of section 4 above (figs 79-80).

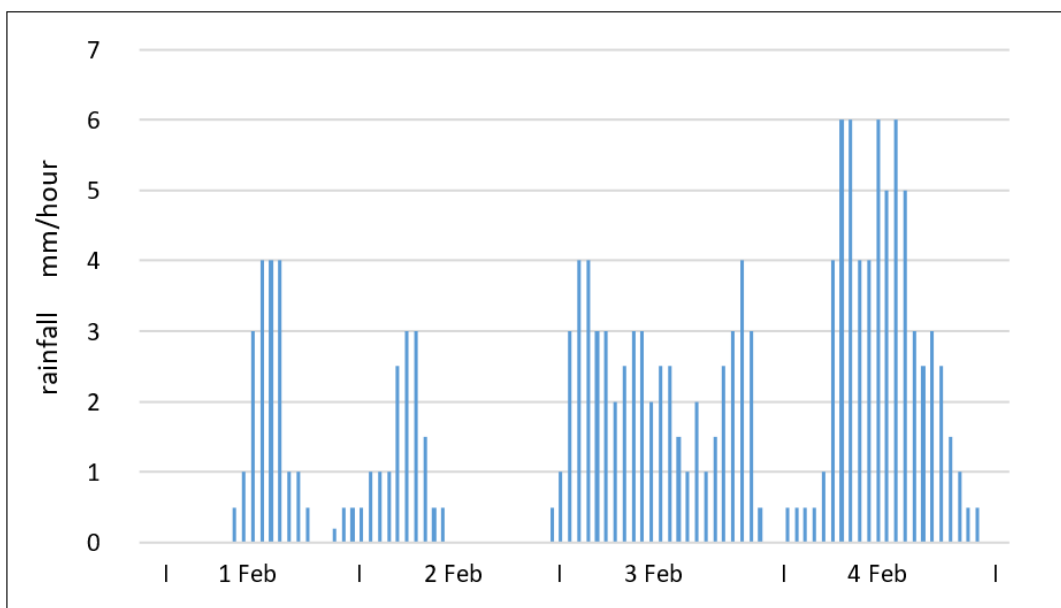


Figure 79: Rainfall in Fairbourne for the extreme storm event of 1-4 February 2004.

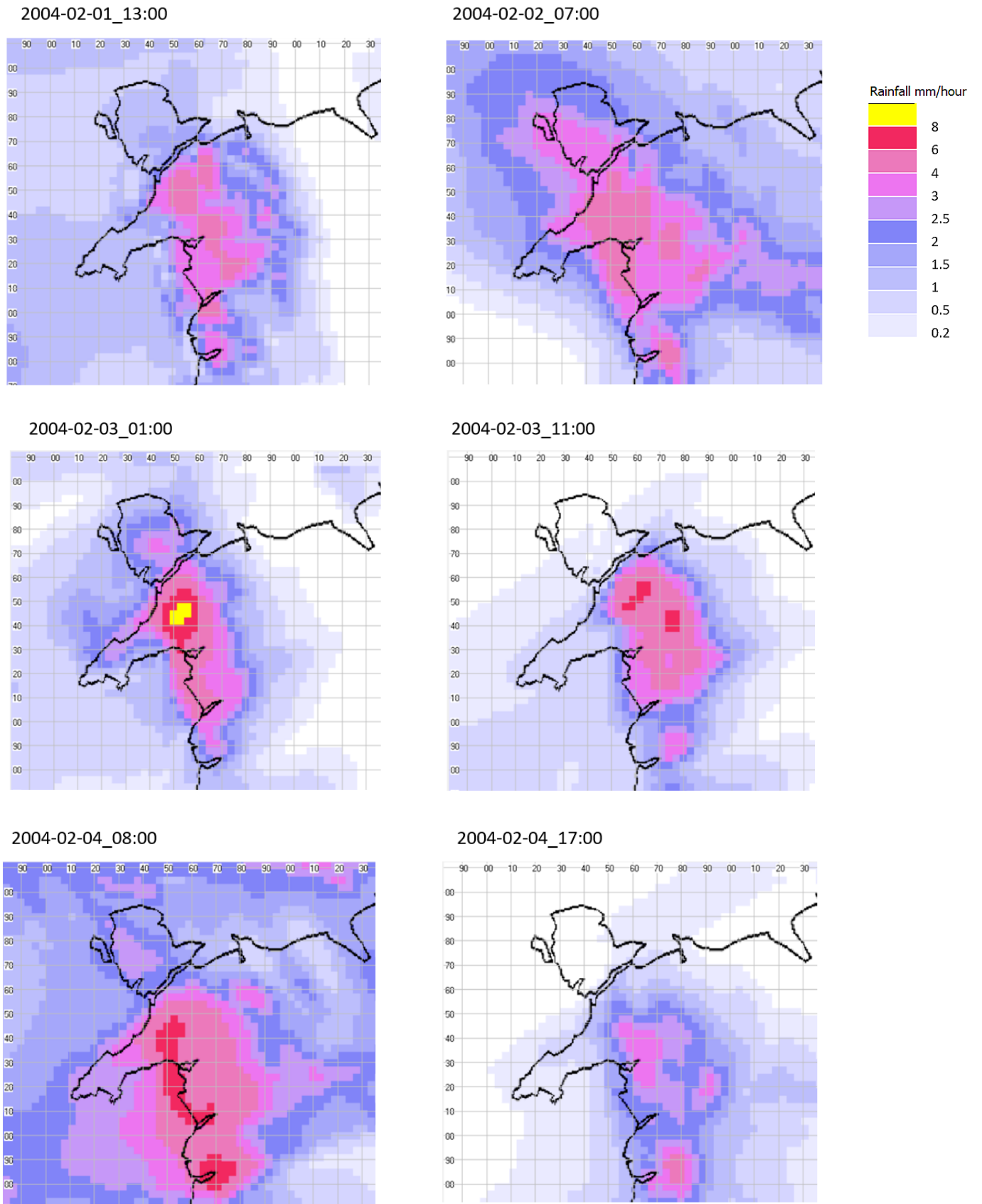


Figure 80: Rainfall distributions during the 1-4 February 2004 storm event.

Hydrographs were produced by the hillslope model for the Afon Henddol and Afon Morfa to specify the river flows which would enter the coastal lowland during the four days of the storm event. This water must flow across the lowland area to discharge into the Mawddach estuary through the tidal gate near Morfa Mawddach.

The digital elevation model for the coastal lowland is displayed in fig.81. It is seen that the ground generally lies between 3 and 8 metres above Ordnance Datum.

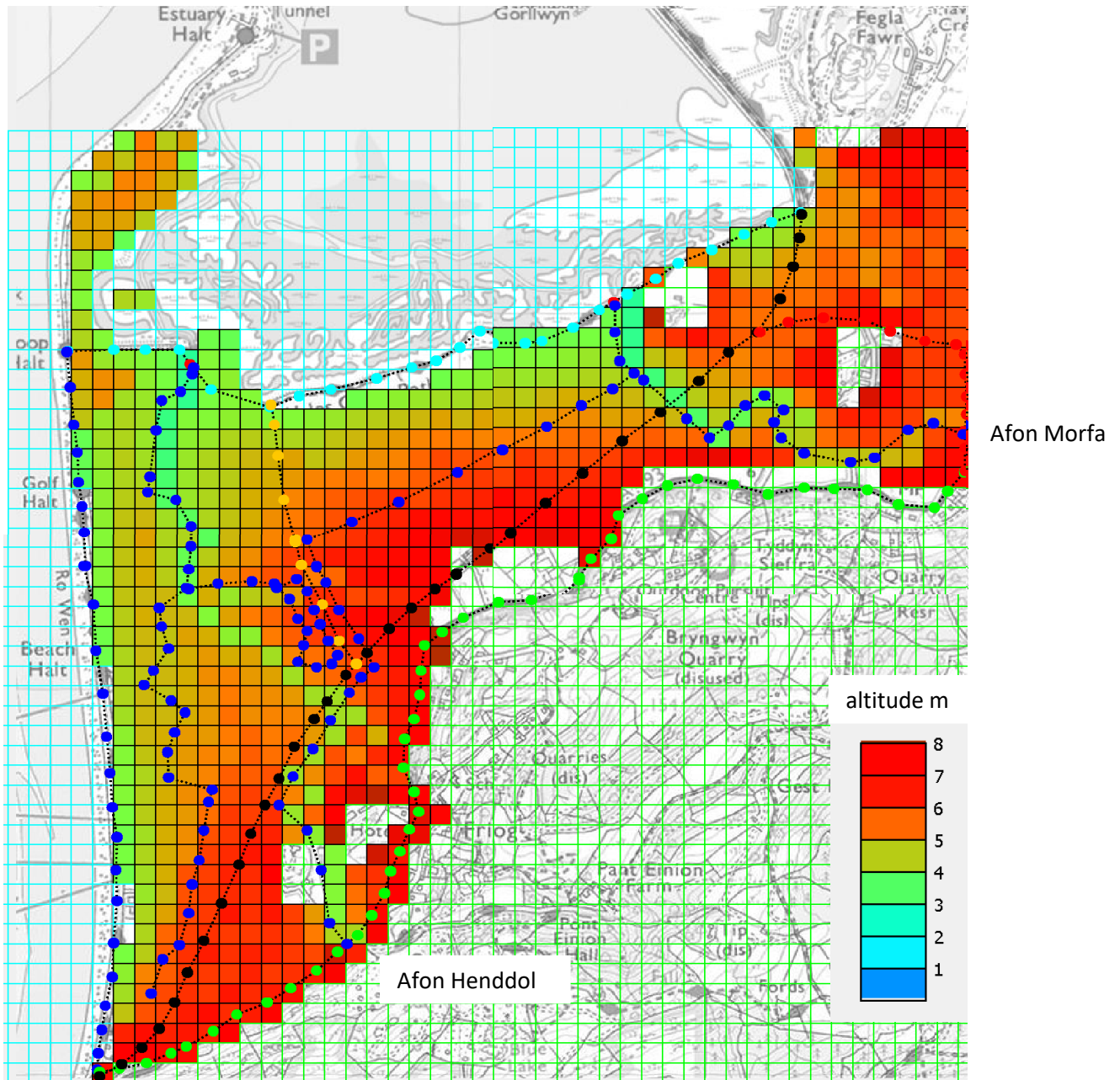


Figure 81: Ground surface elevations for the coastal lowland around Fairbourne.

In the east of the map area, the Afon Morfa is seen to follow a shallow valley as it descends slightly to the tidal gate.

In the west, the Afon Henddol again begins its descent in a shallow valley, but has been re-routed as it approaches Fairbourne village. It appears that the original course of the river continued northwards alongside Glan y Mor, where it now forms a drainage ditch (fig.82). The current course

of the Afon Henddol continues alongside the railway to a culvert beyond Fairbourne station, then turns northwards to reach the tidal gate near Fairbourne golf course. In the proposed flood protection scheme, the Afon Henddol would be re-routed eastwards away from the village to join the Afon Morfa.



Figure 82:
Probable former course of the Afon Henddol, now marked by a drainage ditch. Glan y Mor, Fairbourne.

It is important to determine the gradients of the rivers and drainage ditches, to determine whether an adequate flow towards the estuary tidal gate will be maintained under storm conditions. Long profiles of water channels draining the coastal lowland are shown in fig.84.

The Afon Morfa descends from the hills above Ynysgyffylog, then crosses fields at a very gentle gradient to reach the estuary. For part of its course, the river meanders in large loops (fig.83). It is known that the Afon Morfa regularly floods after extended periods of heavy rainfall.



Figure 83:
Afon Morfa crossing fields to the west of Ynysgyffylog.

The Afon Henddol descends from hills above Fairbourne, follows a circular route around the village, then crosses the coastal lowland to the tidal gate near Fairbourne golf course. The river gradient is very gentle and a risk of flooding exists. The banks of the river were raised during the 2016 flood alleviation scheme along the sections to the south and east of Fairbourne village.

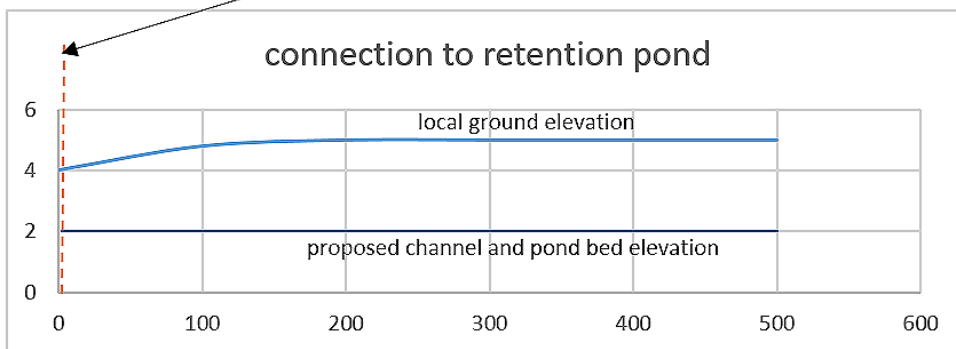
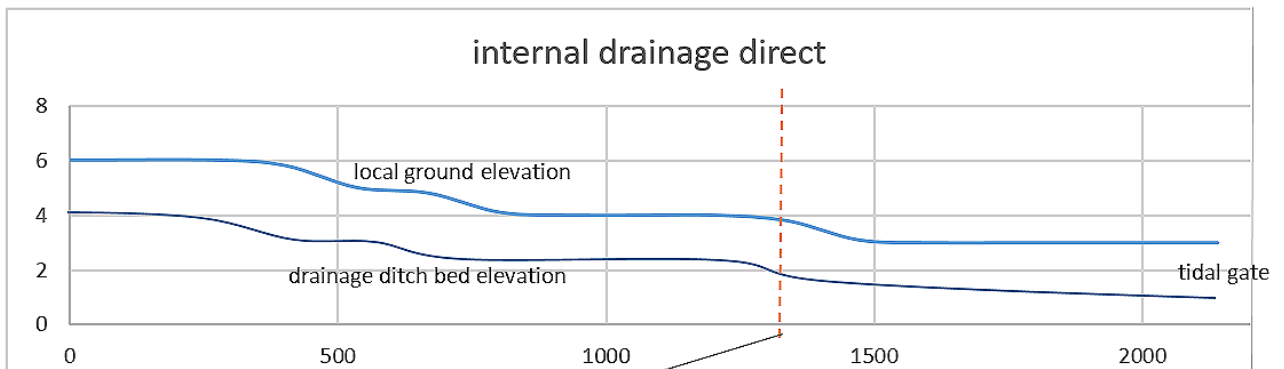
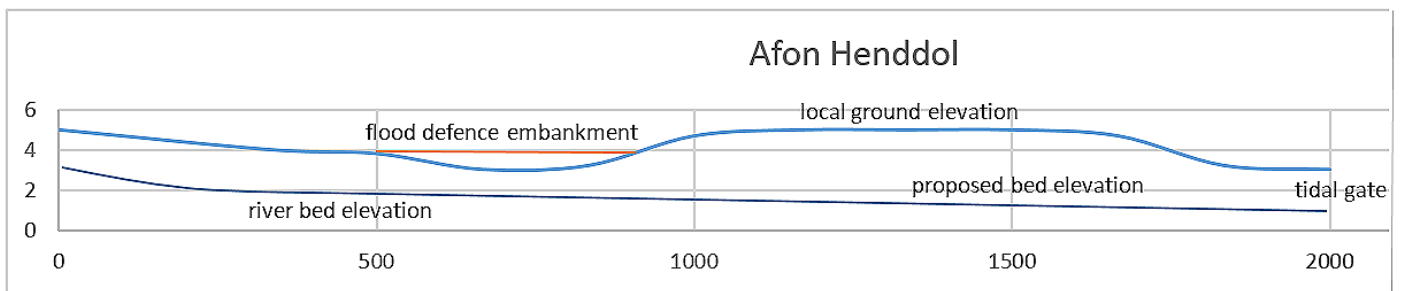
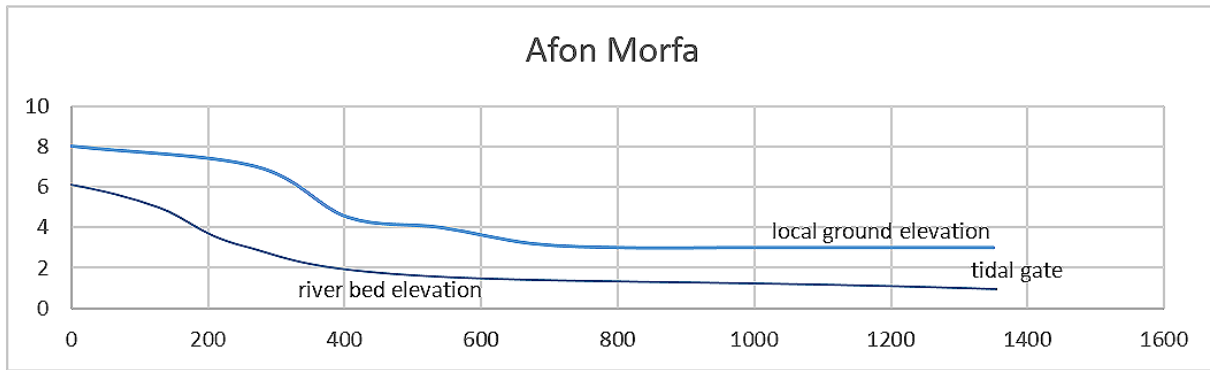


Figure 84: Long profiles of the current and proposed water courses draining the coastal lowland.

The design specification for the Afon Henddol flood embankments is shown in fig.85, along with a view of the river as it appears in December 2021. It is evident that the river is now modifying its channel as it erodes into soft sediment, although the embankments remain stable.

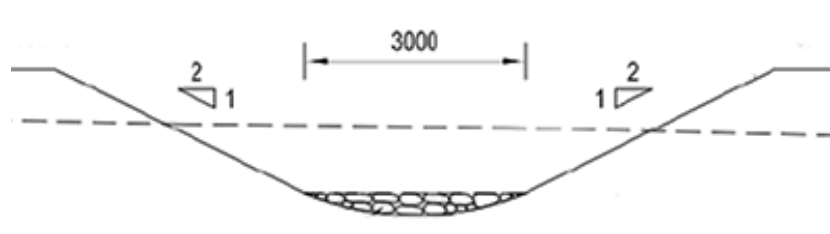


Figure 85:

Afon Henddol near Fairbourne railway station

(above) Design specification for flood alleviation works.

(below) River channel, bounded by flood embankments.



In the proposed flood protection scheme, the Afon Henddol would be re-routed outside the boundary formed by a new embankment to the east of Fairbourne village, and would cross the coastal lowland to join the Afon Morfa.

A drainage ditch network exists within the proposed Fairbourne flood protection area. The direct route to the tidal gate descends at a very gentle gradient (fig.86).

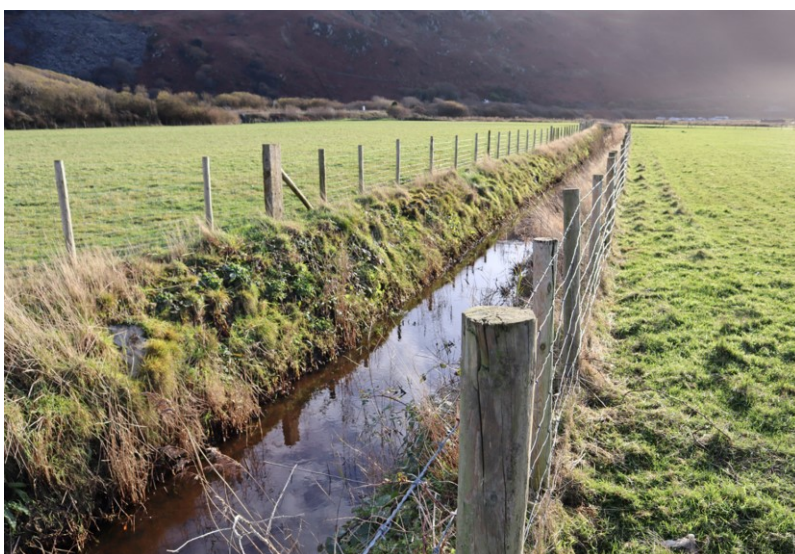


Figure 86:

Drainage ditch crossing fields to the south of Fairbourne village.

A branch from the direct route provides access to the proposed flood water retention pond, where water can be stored when the tidal level temporarily prevents discharge to the estuary.

The rivers and drainage ditches around Fairbourne village generally have a slow, steady flow due to the very gentle downstream gradient, and are straight for much of their course. It is therefore convenient to use the Manning equation to model the flow through the drainage system, rather than the more complex kinematic wave equations required to model the turbulent flows of the estuary and mountain streams.

The Manning formula uses the water surface slope, cross-sectional area and wetted perimeter of a length of the channel, to determine the flow rate:

$$Q = \frac{KAR^{2/3}S^{1/2}}{n}$$

Q is the flow rate, measured in metres/second.

A is the cross sectional area of the water flow, in square metres.

R is the hydraulic radius, calculated as the cross-sectional area of the water flow divided by the wetted perimeter where the water flow is in contact with the channel floor and sides. The hydraulic radius is measured in metres. Calculations for the model are based on the channel profiles shown in figs 83, 85 and 86 above.

S is the slope of the water surface at the point of measurement, calculated as a ratio: metres/metre. This is determined according to the long profiles given in fig. 84.

n is the surface roughness, and is based on the channel material and condition. Typical values for channels cutting through soft sediment are:

Earth channel - clean	0.022
Earth channel - gravelly	0.025
Earth channel - weedy	0.030

Appropriate values for **n** will be used, according to the appearance of each section of channel.

K is a constant dependent on the units of measurement, which for SI units is simply 1.0.

Water enters the coastal lowland by river flow, and also by direct storm rainfall onto the land. The model simulates the release of soil water into the drainage system, and the movement of water through the channel network to the tidal gates, making use of the Fairbourne flood water retention pond when necessary.

Wave overtopping of the storm beach and sea wall is applied at Friog for the periods of one hour before and one hour after high tide. An upper limit for the volume of overtopping waves was estimated to be 8,000m³, and this volume is added to the drainage ditch system south of Fairbourne village during the appropriate time period.

A final stage in the model is to simulate the operation of the tidal gates. Drainage outflow occurs at an elevation of 1m above Ordnance Datum, which represents 1m above the mean tidal level measured in Newlyn, Cornwall. This is close to the mean tidal level at Barmouth. Allowance will be made for a rise in mean sea level of 0.5m by the year 2065. It is, however, still safe to assume that the Mawddach tidal gates will be able to discharge for six hours in the lower half of each tidal cycle, followed by six hours when outflow is prevented.

The structure of the hydrological model is shown in fig.87. This begins by initialising the water levels in the rivers, drainage ditches and soils to typical winter values.

The simulation of the four day storm event then begins. Calculations are carried out for each 10 minute period. Rainfall is applied, and soil water levels are adjusted. This process takes account of the slow groundwater movements which occur below the sea wall and estuary embankment in response to tidal height. Surface water and soil throughflow are discharged into water courses.

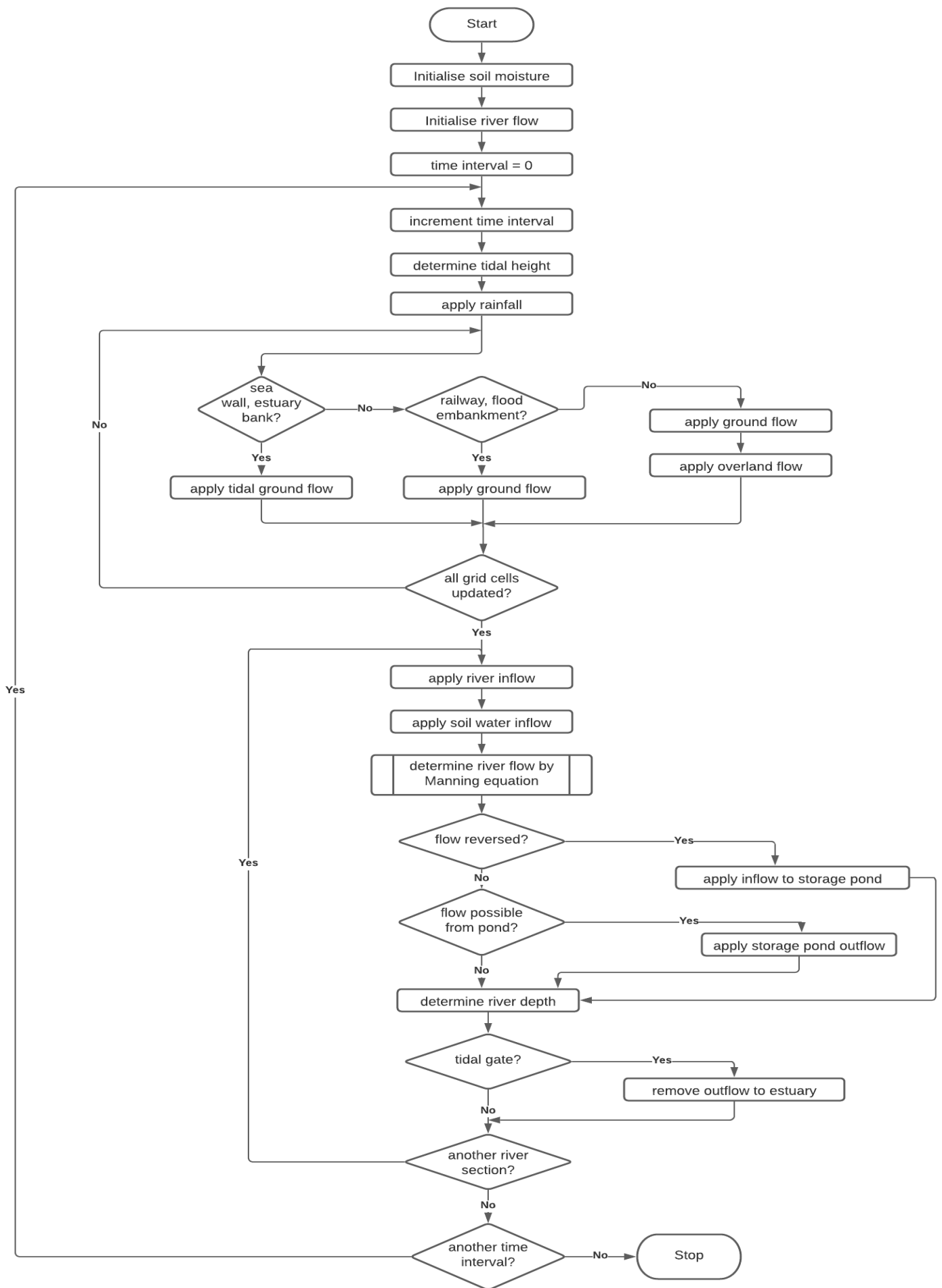


Figure 87: Structure for the coastal lowland hydrological model.

Water flow for each channel segment is calculated, and the appropriate water volume transferred downstream to initialise the next time interval. Water depths within the channel are found, and any overbank flooding identified.

Water arriving at either of the tidal gates is discharged into the estuary if tidal conditions permit. At periods of high tide, the Fairbourne drainage network will fill until water overflows along the connecting channel to the interception pond. When the tide falls again, water returns from the interception pond to the tidal gate. Flows along the connecting channel are calculated.

At the end of the time interval, a map displays the water table depths across the coastal lowland so that any areas of surface water flooding are identified (fig.88).

The modelling calculations are repeated for each subsequent time interval until the storm event period is completed.

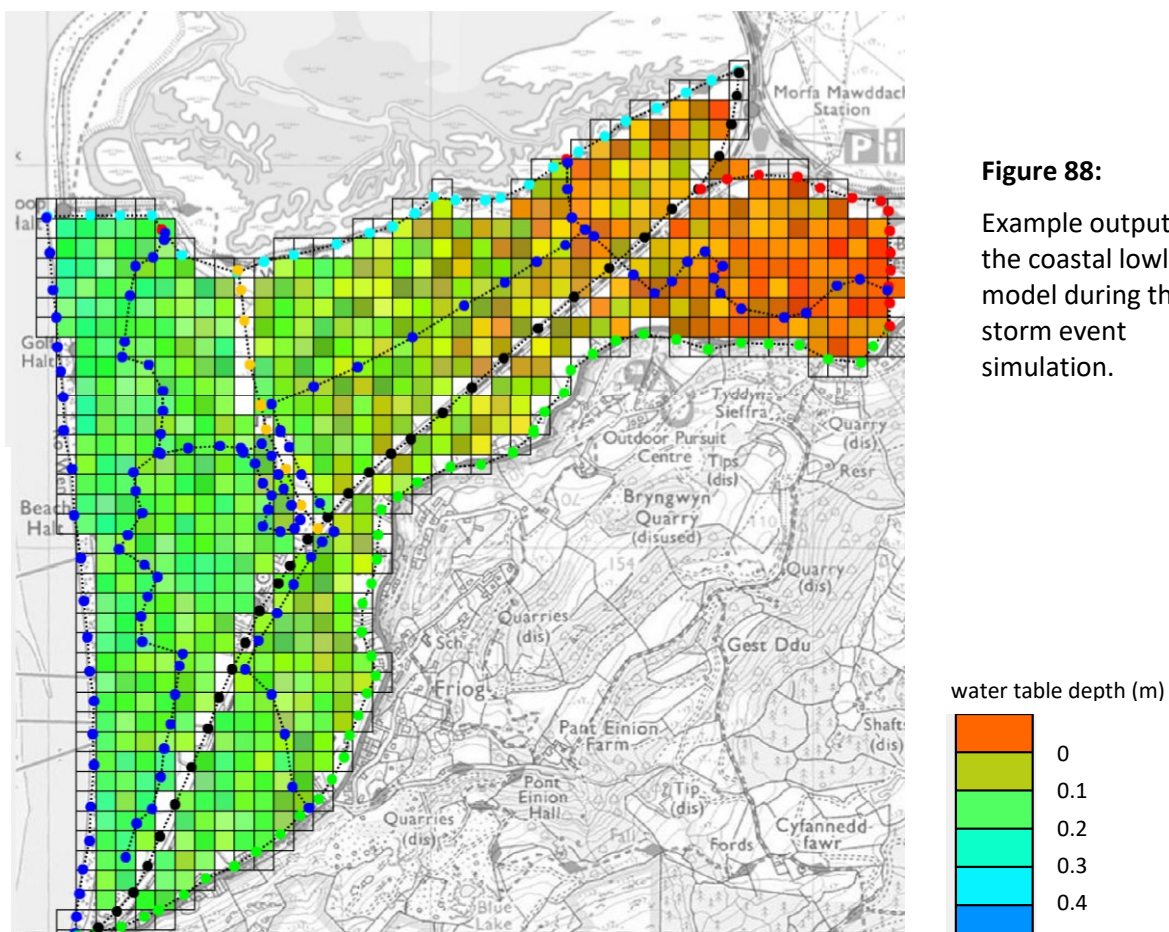


Figure 88:
Example output from the coastal lowland model during the storm event simulation.

Modelling indicates that no surface water flooding occurs in Fairbourne village during the storm event, and the volume of drainage water can be contained within the drainage ditches and retention pond, with discharge to the estuary in the lower part of the tidal cycle.

Some surface water flooding is indicated for the area around the course of the Afon Morfa in the east of the area. Monitoring of the Afon Henddol around Fairbourne indicates that water flows are contained within the channel and no overbank flooding occurs.

7. SUMMARY

This investigation found no convincing scientific justification for abandoning and demolishing Fairbourne village, either before or after the year 2065. Where flood risks were identified, these could be managed in simple and cost effective ways without disruption to the village.

It is reasonable to assume a maximum increase in mean sea level at Fairbourne of 0.5m up to the year 2065. A maximum off-shore excess wave height above specified tidal height of 6m at Fairbourne is a reasonable assumption.

It appears very unlikely that the water height against the estuary flood embankment at Fairbourne could exceed the combined tidal and flood surge height at the estuary mouth. Sea waves rapidly dissipate within the enclosed and sheltered waters of the estuary, particularly during shallow tidal flow across the extensive salt marsh.

It is predicted that the maximum water height against the Fairbourne embankment for the year 2065 would be produced by a maximum 6m spring tide combined with a maximum storm surge of 2m, giving a total of 8m above chart datum. Surveying indicates that the height of the Fairbourne embankment is above this predicted maximum water level, but the freeboard of 0.4m is small. It would be advisable to raise the height of the section of flood embankment north of Fairbourne village by 1m as a precautionary measure at some time before 2065.

Hillslope runoff modelling for a worst case storm extending over a period of three days produced an estimated maximum discharge of 3m³/sec. for each of the rivers Henddol and Morfa.

The safety of the sea wall along the Ro Wen shingle spit was considered. It is apparent that marine erosion is taking place at Friog corner, although there is no current danger to the coastal defences at this point. It was noted that the landward side of the shingle embankment had been cut back at this point to provide an area of flat ground in front of a group of huts. It is recommended that this shingle be replaced, in order to strengthen the storm beach and sea wall structure.

Further north, the shingle spit is generally stable or slightly increasing in volume. The storm beach is of considerable width and height, so there is negligible risk of the structure being breached during a storm.

Modelling predicts some wave overtopping at Friog in the event of a maximum storm surge corresponding with a maximum spring tide. Overtopping is restricted to a period of one hour before and one hour after high tide. Overtopping rapidly decreases northwards, and is negligible in front of Fairbourne village. An upper estimate for the volume of sea water overtopping the embankment during a storm is 8,000m³, representing a peak flow into the Fairbourne drainage network of 2m³/sec.

Overtopping waves may cause some erosional damage to the landward face of the embankment south of Fairbourne village. Overtopping could be reduced in several ways: by increasing the height of the sea wall by perhaps 1m at affected locations; or by encouraging deposition of beach sediment through construction of an off-shore reef or installation of groynes. Alternatively, the landward surface of the embankment could be protected from erosion by addition of a layer of shingle and installation of a land drain.

A hydrological model has been constructed to determine whether the proposed flood protection scheme for Fairbourne would be able to safely handle storm water discharge. A worst case storm event was modelled, based on climate change predictions for the year 2065. Modelling indicates that no surface water flooding occurs in Fairbourne village during the storm event, and the volume of drainage water can be contained within the drainage ditches and retention pond, with discharge to the estuary in the lower part of the tidal cycle.

Some surface water flooding is indicated for the area around the course of the Afon Morfa in the east of the area. Monitoring of the Afon Henddol around Fairbourne indicates that water flows are contained within the channel and no overbank flooding occurs.

It must be stated that the models used in this project are subject to significant uncertainty in predicted sea level, storm surges and storm rainfall, although plausible worst case scenarios have been chosen. Errors in predictions will inevitably occur, although these has been kept to a minimum by calibrating models against measured field data wherever possible. It is, however, important to continue regular monitoring of flood responses to storms at Fairbourne, and to take prompt remedial action if unforeseen problems should arise. In particular, the internal drainage of Fairbourne village should be monitored, to identify if pumping becomes necessary to reduce the water table under extreme storm conditions.

REFERENCES

- Ahmadian, R., Morris, C., & Falconer, R. (2010). Hydro-environmental modelling of off-shore and coastally attached impoundments off the north wales coast. In *First IAHR European Congress, Edinburgh*.
- Arthog Community Council (2021). Analysis of Community Awareness Questionnaire response. www.cyngorarthogcouncil.cymru.
- Bricheno, L. M., Wolf, J., & Aldridge, J. (2015). Distribution of natural disturbance due to wave and tidal bed currents around the UK. *Continental Shelf Research*, 109, 67-77.
- Buss, S. (2018) Fairbourne: modelling future risk of groundwater flooding. Stephen Buss Environmental Consulting Ltd, Shrewsbury.
- Deltares (2017). Delft3D modelling of storm surge during a hypothetical hurricane in the Irish Sea. YouTube.
- Hall, G. (2008). An Integrated Meteorological / Hydrological Model for the Mawddach Catchment, North Wales. PhD Thesis, Bangor University.
- Howarth, M. J. (2005). Hydrography of the Irish Sea. In *SEA6 Technical Report*. UK Department of Trade and Industry's offshore energy-Strategic Environmental Assessment programme.
- Larcombe, P. & Jago, C. F. (1994). The late devensian and holocene evolution of Barmouth Bay, Wales. *Sedimentary geology*, 89(3-4), 163-180.
- Owen, K. (2010) Fairbourne flood alleviation scheme: ground investigation programme report no. 877. Environment Agency.
- Phillips, M., Thomas, T., Morgan, A. (2017) Flood and Coastal Erosion Risk Management: Fairbourne Going Forward coastal processes, beach profiles and aerial photographs assessment of change. University of Wales Trinity Saint Davids.
- Pu, J. H., & Shao, S. (2012). Smoothed particle hydrodynamics simulation of wave overtopping characteristics for different coastal structures. *The Scientific World Journal*, 2012.
- Pullen, T., Allsop, N. W. H., Bruce, T., Kortenhuis, A., Schüttrumpf, H., & Van der Meer, J. W. (2007). EurOtop wave overtopping of sea defences and related structures: assessment manual.
- Thompson, D. A., Karunaratna, H., & Reeve, D. E. (2017). Modelling extreme wave overtopping at Aberystwyth Promenade. *Water*, 9(9), 663.
- UK Government. 2014. UKCP09 Climate change projections [Online]. Available: <http://ukclimateprojections.metoffice.gov.uk/23189>